CHIMIA 42 (1988) Nr. 11 (November)

Metal Clusters: Between Atom and Bulk**

Ernst Schumacher*
and his present team:
Fritz Blatter, Martin Frey, Uli Heiz, Ursula Röthlisberger, Martin Schär, Arthur Vayloyan, and Chahan Yeretzian

The basic question of metal cluster research is the following: How do the macroscopic metallic properties – conductivity, optical lustre, chemical and catalytical reactivity, magnetism, malleability and ductility – evolve as a function of cluster size starting from the electronic states of the atom? It turns out that in a cluster of 20–40 atoms most of what we acknowledge as «metallic» is already fully developed.This is the reason why the beautiful chemistry of metal cluster complexes *has not contributed to an understanding of the transition from the atom to the bulk: The chemical interaction of the ligands (e.g. CO, C_5H_5, PR_3) with the core of metal atoms dominates electronic and structural properties to the extent that the underlying laws of metallic conduct are completely masked. We have, instead, to investigate* bare *metal clusters. This is, however, impossible with the traditional tools of inorganic chemistry. High temperature methods, molecular supersonic beam technology, manipulation in vacuum systems, laser spectroscopy, mass spectrometry, and low (and high) temperature matrix isolation experiments are necessary. Furthermore guidance of the experimental work by quantumchemical calculations, molecular dynamics simulations, and the combination of the two are important because «chemical intuition» does not lead far in a field where chemical thinking has barely begun to develop: The molecular science of metals! – In this article we present the experimental environment of metal cluster work and then concentrate on the results available: stability of cluster sizes, selectivity of the heterometallic bond, electronic and magnetic properties from the atom to the bulk, insulator-metal transitions, size-dependent chemical and catalytic properties. Global, quantumchemical and ab initio molecular dynamics models are discussed. This leads to the last question of chemical interest: Why do metal clusters not have shape, or if they do, how can it be determined?*

Ernst Schumacher: Born 1926 in Baden, Kanton Aargau. Studied chemistry at the Universität Zürich from 1945; Dr. phil. 1951 with thesis in physical-inorganic chemistry with Prof. Klaus Clusius. Research assistent 1951–1953. Postdoc 1954–1955 with H.C. Urey and M.G. Inghram, University of Chicago. 1955 Habilitation at the Universität Zürich in Inorganic and Physical Chemistry; 1957 Extraordinarius, 1959 Ordinarius and Head of the Institute for Inorganic Chemistry. 1962 Guest professor at the Chemistry Department of the University of California, Berkeley. 1964–1972 Research Director of Ciba-Geigy Photochemical in Fribourg-Marly. Since 1972 Ordinarius at the Institute for Inorganic and Physical Chemistry, Universität Bern. – He likes to think of himself as Professor of Chemistry since he has always tried to learn those fields of chemistry, physics, and mathematics which were relevant for his chemical research problems without recognizing the canonical obstacles between the disciplines. He has also served various research funding institutions, advisory committees of MPI's and scientific journals, and as consultant to several chemical and photographic companies. He has a honorary degree from the Université de Fribourg.

1. Cluster Science

The evolution of the topological dimension[1] D from the atom with D = 0 to matter in bulk with D = 3 trivially passes through a state where D = 2, hence with «surface»-dominated properties. Most of cluster research is directly or indirectly concerned with the consequences of a non-

* *Correspondence:* Prof. Dr. E. Schumacher
Institut für Anorganische und Physikalische Chemie
Universität Bern
Freiestrasse 3, CH-3012 Bern

** After talk given at the fall meeting of the Swiss Chemical Society in Bern, October 21, 1988. Support of our research by the Swiss National Science Foundation (grant 2.348-0.86) is acknowledged.

negligible 2-dimensional boundary or inhomogeneity of the observed system.

Clusters have first been defined by *Robert Boyle*[2] (Fig. 1) as «little primary concretions of minute particles not easily dissipable into such particles as composed them». We would now add the attribute of lacking closure, i.e. *clusters* differ from *molecules* or *complexes* by their ability to grow to arbitrary size provided a suitable environment is available supplying the «minute particles as composed them». This description implies unsaturation and reactivity. The preferred environment which strictly prohibits growth yet does not influence the already formed stable clusters beyond unshieldable electromagnetic effects is a very good vacuum. Hence this must be the medium for observing clusters as free particles unharmed by solvents, matrices, or ligands. However, once their properties established we shall not hesitate to expose them to all sorts of interactions in order to learn about size-dependent properties. Methods have been developed to make large quantities of clusters with narrow size distributions or nearly monodisperse particles. Their unusual properties give promise for new devices and materials, «cluster materials»[3].

Since several years we have been interested in free metal clusters[4]. The motivation for choosing «concretions» of atoms from *metallic elements* is the intuition that metals more than any other category of matter should exhibit drastically changed properties compared to bulk when dispersed to the molecular level. Similar ideas have led others to form a large, very active community of scientists[5]. Apart from inorganic, physical, and theoretical chemists many come from condensed matter and metal physics, including theoreticians, and from corporate research[6]. Hence, the cluster field has served to bring together different disciplines with varying paradigms, a cause for stimulating exchange of ideas and also for lively controversies[7].

Of course, there are other uses of the term *cluster* than the description given. Apart from the well-known *metal cluster complexes*[8] – ligand covered, usually highly symmetrical metal cores now advanced to the 5-shell icosahedron with 561 Au or Pd atoms (which shows «metallic» properties)[9] – any polynuclear moieties in crystals are called clusters, e.g. «heteropolyanions» like polyvanadates with distinct V^{IV} and V^{V} [10].

It ſeems not abſurd to conceive that at the Propoſ. I.
firſt Production of mixt Bodies, the Univerſal Matter whereof they among other Parts of the Univerſe conſiſted, was actually divided into little Particles of ſeveral ſizes and ſhapes variouſly mov'd.

Propoſ. II. *Neither is it impoſſible that of theſe minute Particles divers of the ſmalleſt and neighbouring ones were here and there aſſociated into minute Maſſes or Cluſters, and did by their Coalitions conſtitute great ſtore of ſuch little primary Concretions or Maſſes as were not eaſily diſſipable into ſuch Particles as compos'd them.*

Fig. 1. Two of the famous four propositions which Robert Boyle advanced in «The Sceptical Chymist», 1661, to build a scientific basis for chemistry as distinct from the «Spagyrist's hypostatical principles as they are wont... by the Alchymists». London, Cadwell, MDCLXI. Facsimile reproduction, Dawson, London (1965), p. 37–39.

2. Metal Clusters

This term implies «metallic» character. A more accurate name would be «atom clusters from metallic elements» since the very question whether they are *metallic* and which observables would reveal this property is our first research object. Since *Pauling's* endeavours to give a chemical theory of the metallic bond[11] chemistry has left this field entirely to the condensed matter physicists. Most texts of quantum chemistry do not even have a chapter on metals. At most they treat as a warm-up exercise the independent particle model in a 3-dimensional box with infinite walls, *Sommerfeld's* electron gas description of a metal which in pre-quantum times *Lorentz* had already anticipated. This is also one of the starting points for the metal physicist to treat a *finite piece of metal*. However, he then quickly chooses a much more convenient boundary condition: The periodicity of a 3-dimensional ideal lattice of atomic cores stripped of their valence electrons. This offers the possibility to solve *Schrödinger's* equation for the motion of the electrons in the reciprocal lattice and leads by virtue of the translational symmetry to the band structure of an infinite crystal[12]. Every sharp energy level of the $N(\rightarrow\infty)$ assembled atoms has now spread to a finite width of N contiguous $(\rightarrow\infty)$ levels. These bands are separated by gaps or forbidden regions from their neighbours of different atomic parentage if required by symmetry restrictions. In this model metals are distinct from other solids in that they have a *partially filled* topmost energy band, the *conduction band*. At 0 K the highest occupied orbital, the HOMO, marks the Fermi level. Above this level a large number of infinitesimally separated empty levels exist which can be easily populated even at very low temperature. Since the orbitals are delocalized on the whole crystal the predominant single occupation of levels above and slightly below the Fermi level at finite temperatures creates electrons unlocked from the Pauli exclusion principle and hence with essentially no constraints on their motion. They are free to react e.g. to the force exerted by an external electric field. They also create the observed finite magnetic susceptibility, the so-called Pauli paramagnetism of metals since they tend to acquire an unbalance of $\uparrow$ and $\downarrow$ spins (*Hund's* rule).

This very successful theory has recently partially collapsed when it was discovered, that crystalline, quasi-crystalline, amorphous (glassy), and even liquid metals (all of the same chemical composition) exhibit similar metallic properties even though the range of «periodicity» is reduced from essentially infinity to two or three radial shells around a certain atom (in a statistical sense and not stable in time with liquids)[13]. Moreover, it appears to be tenuous to describe single atom «impurities» or the perturbations by the surface boundary in a small, finite piece of metal in the framework of a theory whose validity is strictly limited to a surface-less infinite ideally periodic structure. The same collapse of a paradigm happened when amorphous semi-conductors worked almost as well as the crystalline variety for which the theory applies.

Now, the transient «species» of aggregation in a liquid metal or the average scale of order in a glassy metal has a size of a dozen to several dozen atoms[14], just the range in which we study metal clusters. Therefore, understanding clusters as building blocks and how they couple to form a macroscopic system becomes a central issue for the development of consistent models of the predominantly low-ordered (often high-surface) materials of our natural and technical environment. Obviously, this statement is not limited to metallic matter.

3. Making and Characterizing Metal Clusters

The simplest and best understood bulk metals are formed by group 1a and 1b (or 1 and 11) elements. From these and all other metals it has become easy to prepare clusters of practically any size. Their formation can be achieved by dispersion of the bulk or by aggregation starting with atoms. We concentrate on the latter methods: The creation of metal atoms

requires several chemical high-temperature techniques which become the more sophisticated the more refractory the metal is. For the low-boiling alkali metals, and for the 2b (12) group, then Mg, Yb, Sr, Eu and perhaps Mn (in the order of increasing boiling point), which all have a closed ns^2 shell of the atom ground state, thermal vapourization of the bulk metal creates partial pressures of several dozen to hundreds of mbar at temperatures below 2000°C. This can be reached by conventional electrical furnaces with radiative heating and proper shielding of the capsules containing the metal(s)[15]. It is also possible to use chemical reduction of halides or oxides of a more volatile metal with a less volatile one. For example, very pure potassium beams can be produced with {KCl} and {Ca} granules since the product $\{CaCl_2\}$ has a much lower vapour pressure than K[16]. This economizes on the otherwise very expensive pure potassium. Finally there exist several thermolytical processes like dissociation of azides[17], of oxides e.g. for Zn, Cd, Hg production, and other salts.

The atomic vapour now has to be induced to form the clusters. This may be realized as equilibrium process in a closed system in the presence of the condensed phase: The higher the temperature and thus the saturation pressure the more complex the gas phase species become. They can be extracted and probed by a small effusive hole. This *Knudsen* type cluster source has been mainly used for producing homo- and heteronuclear dimers of practically all metallic elements[18]. Some higher aggregates have been studied especially for Li and Na, Li_5 being the largest so far[19]. One important result from these experiments, not easily got from any other, is the enthalpy of formation of each cluster. The method runs into difficulties for larger clusters because the Knudsen condition for equilibrium effusion can no longer be fulfilled if the vapour pressure becomes too large: It requires that the probe orifice be small compared to the mean free path of the particles in the closed system and that the leakage does not change the equilibrium composition. The first condition is much more severe than the latter and prevents the study of clusters large enough to be really relevant for the main topics of cluster research, i.e. observing the transition from the atom to the bulk.

The main vehicle for free cluster studies is the supersonic nozzle beam: The nozzle is typically a small tube of between (0.01–) 0.05 to 0.4 mm diameter with a length comparable to the diameter. On one side of it is the atomic vapour with a stagnation pressure of a few hundred mbar, on the other a pressure of less than 10 µbar. Under these conditions the device is a thermomechanical transformer: The nozzle throat forces a viscous mass flow at about the average thermal speed of the hot gas in the flow direction with only minor lateral motion. At the orifice this expands into the vacuum retaining largely its linear momentum as mechanical forward thrust of a tightly peaked molecular beam. The small random lateral motion is equivalent to a very low temperature. Within the expansion zone pressure is high enough to create a large number of collisions between the particles. This leads to the aggregation of atoms and growth of clusters as long as the collision regime lasts, about 20 µs or 2–3 cm of flight path. The collisions also create a broadening of the molecular beam which is corrected by applying «skimmers» and collimating slits in successive pumping stages. The adiabatic or isentropic expansion causes drastic cooling which induces supersaturation, nucleation, and then condensation of molecular droplets – to phrase the same events in thermodynamical terms. However, thermodynamic equilibrium is never obtained in this process. Control of the cluster formation is linked to the variables: throat diameter, stagnation pressure, nozzle geometry and the admixture of auxiliary («seed») gases, usually noble gases, which do not (normally) attach themselves to the metal clusters but take part in the expansion process and collisional cooling of the clusters *in statu nascendi*. Of course, nozzle beam expansion has been mathematically modelled and can be described in precise terms[20]. The mechanical motion of a beam element is very much faster in the laboratory frame of reference than the average random motion of its particles with which a temperature and hence a sound velocity can be associated. Hence, the beam is supersonic with Mach numbers easily as high as 20 to 40. The supersonic beam has a number of uniquely pleasant properties: All its particles move approximately with the same velocity vector *independent of mass*, which creates a so-called collisionless environment (*Zare* et al.[21] discussed the validity of this assumption); the beam shows only a small divergence of the strong forward peak and thus offers a high particle density for experiments with the beam particles and at the detector located somewhere downstream. In Fig. 2 a typical molecular beam machine for cluster formation, handling and detection is shown, and in Fig. 3 the evolution of the mass spectra of sodium clusters is demonstrated when the Ar seed gas pressure in a constant vapour pressure of Na is continuously increased. We interpret the pattern in Section 5.

For a synthetic inorganic chemist[22] it comes as a shock that we are dealing here with a preparative device which does not allow (without additional hardware[23]) to obtain a single species of cluster. Instead we produce a large number of different particles forming a wide size distribution.

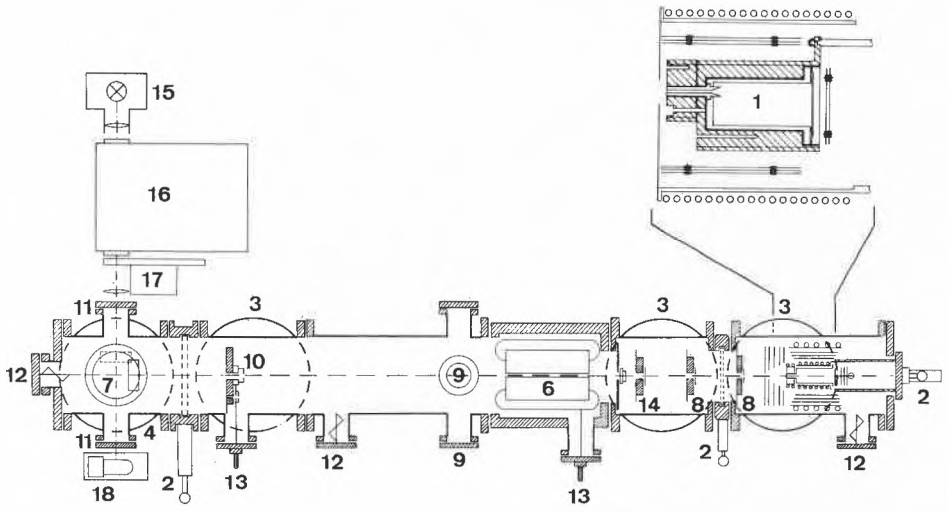

Fig. 2. Schematic of a molecular beam machine, used for metal cluster research[31]*: 1) Metal source capsule in its radiative oven and shield. Left, the orifice with the separate nozzle heater. Tubes for thermocouples; 2) Flange assembly which carries the oven and electrical connections, separators; 3) 2000L Diffusion pumps for three differential pumping stages; 4) Cryopump in the last stage; 5, 6) Stern-Gerlach magnet, or electrical quadrupole, or mass spectrometer; 7) Cryostat with turnable sapphire target for matrix isolation at liquid He temperature; 8) Slit banks for collimation; 9) Optical windows for laser applications and detection of emission at right angles; 10) Langmuir hot wire probe for total beam intensity; 11) Optical path for measuring absorptions of matrix isolated species; 12) Ionization pressure gauges; 13) Electrical feed-throughs; 14) Electromagnetic beam chopper for phase sensitive detection of beam changes; 15) Light source, 16) Monochromator, 17) Light chopper, and 18) Photomultiplier: Spectral photometer for matrix studies. – We have two more beam machines, one for seeded and crossed beams, allowing the study of chemical and catalytical reactions, and one for dissociation experiments equipped with a reflectron, a TOF type analyzer. The three machines allow different sets of experimental studies all essential to understanding metal clusters.*

This is, however, in the best of inorganic traditions: A solution system with many species of complexes can be precisely investigated, although only few or none of the components may be isolated unchanged from the equilibrium mixture[24]. In order to pursue our goal to learn about the properties of the single size particle in a molecular beam environment one uses ionization and mass spectrometric detection, i.e. a separation technique.

The philosophy then is to force any type of observation to modulate the mass spectrometric signal characteristic for only one species. Extracting the modulation from that signal reveals the signature of the property probed by the imposed interaction.

Applying this idea[25] we have learned in the last 10 years to measure among others the following properties in a particle specific fashion:

- relative intensity, mass: This is the (trivial) information given by a straightforward MS scan. In this context the relation between MS *intensity* of an ion with m/z and *abundance* (i.e. partial pressure $\propto$ concentration) of the neutral precursor is, however, far from trivial[26]. Ionization induced unimolecular dissociation can both enhance or diminish a

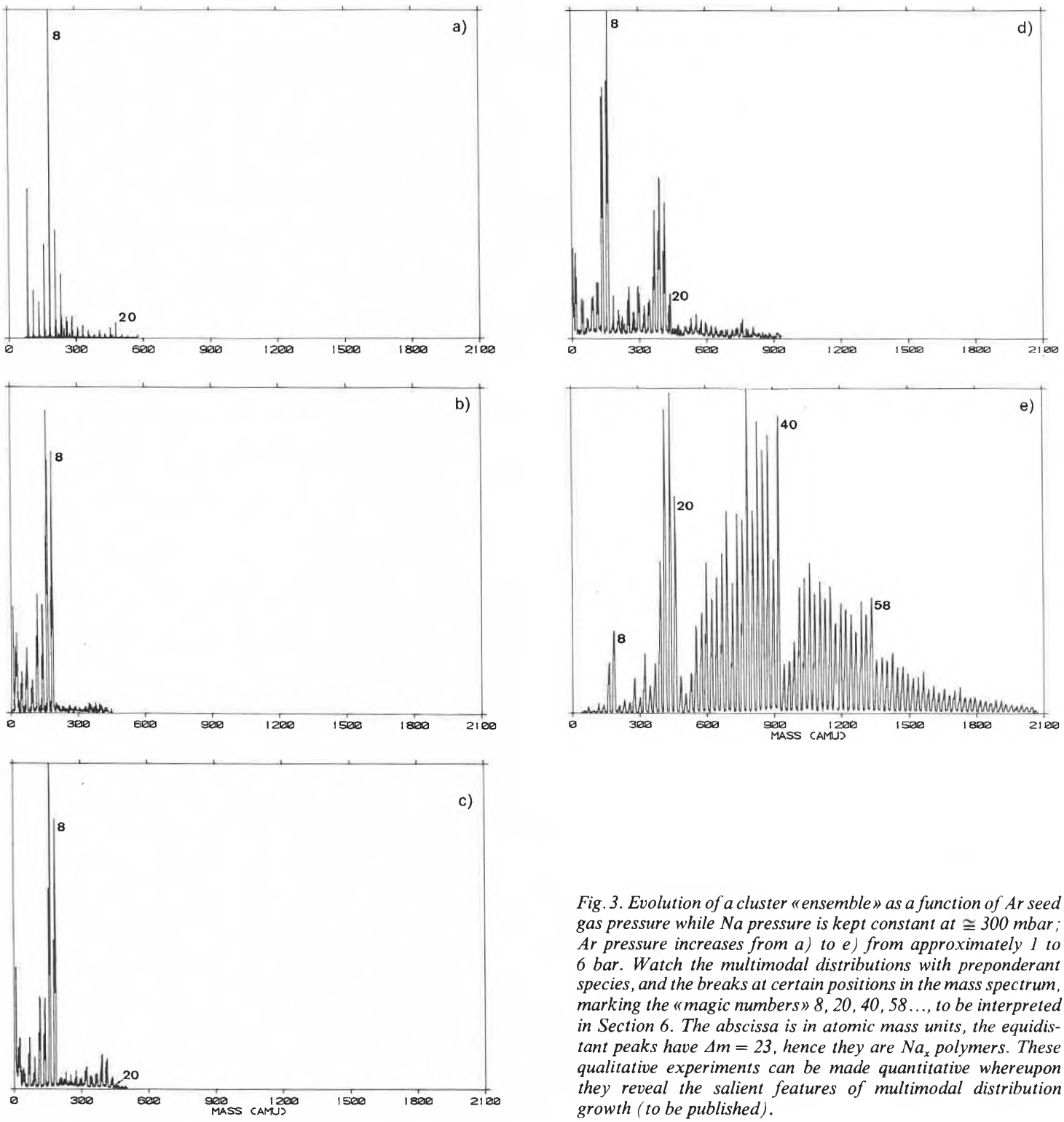

Fig. 3. Evolution of a cluster «ensemble» as a function of Ar seed gas pressure while Na pressure is kept constant at ≅ 300 mbar; Ar pressure increases from a) to e) from approximately 1 to 6 bar. Watch the multimodal distributions with preponderant species, and the breaks at certain positions in the mass spectrum, marking the «magic numbers» 8, 20, 40, 58..., to be interpreted in Section 6. The abscissa is in atomic mass units, the equidistant peaks have $\Delta m = 23$, hence they are Na_x polymers. These qualitative experiments can be made quantitative whereupon they reveal the salient features of multimodal distribution growth (to be published).

given cluster peak. Painstaking analysis of several cluster mass spectra obtained by varying the formation parameters is necessary to eliminate the grossest errors caused by this fact. Much of (metal) cluster literature contains naive interpretations of MS intensity patterns which have not been corrected for fragmentation;
- ionization potentials, electron affinities, and relative cross sections for these processes[27];
- UV/VIS absorption and emission (e.g. LIF) spectra[28];
- IR, Raman spectra[29];
- photoelectron spectra[30];
- magnetic and electric dipol moments[31];
- electric polarizabilities[32];
- individual cluster temperatures[33];
- dissociation kinetics and thermodynamics[34];
- photochemistry[35];
- physi-, chemisorption, and -desorption kinetics and thermodynamics of various reactive and non-reactive molecules[36];
- chemical reactions with non-metallic and other metallic species[37].

This list of properties far exceeds the information one normally has on most species detected in an equilibirium solution mixture. However, one important property is missing here as well as in solution chemistry: the *structure* of the particles. No one has yet found a way to monitor electron diffraction of a molecular beam composed of a mixture of cluster sizes with particle specificity[38]. Electron or grazing angle X-ray diffraction and high-resolution electron microscopy both conventional and with the scanning tunnelling technique on solid *supported* clusters give information on the state of the cluster in a strongly perturbing environment[39]. Hence, they cannot reveal the «true» shape nor that of individual particles. Much weaker but similar reservations exist towards the structures modelled after EPR-experiments on clusters captured and frozen out in a low-temperature argon matrix[40b]. Our hope of obtaining structure information by analyzing the rotationally resolved electronic spectra has only come true to date for M_2 and M_3 particles (see Section 4). Of course, stable metal cluster complexes have been crystallized and X-rayed by the hundreds and produced beautifully bizarre structures. Unfortunately they bear practically no relation to what we indirectly have learned about the structures of free clusters. We will come back to the structure problem at the end.

Cluster generation from metals boiling above 2000 °C needs other high-temperature techniques: The most popular has become laser pulse evaporation from a slowly revolving metal rod or disk[41] (Fig. 4). This creates a hot metal vapour plasma which is quenched by a noble gas pulse, whereupon it nucleates and grows clusters. These are expanded through a nozzle into vacuum as above and then investigated similarly. This technique allows to make clusters from any material including graphite[42], B, Si, SiC, Ge, GaAs, Mo, and W[43]. We have used it to prepare highly active heterogeneous catalysts from group 8 elements[106].

Other «high energy» techniques use fast atom or ion bombardment or sputtering of metal targets with noble gas ions[44]. These sources produce very hot, usually cationic clusters unless cooling by collisions and charge neutralization is applied. There is also no practical limit at what materials these methods may be directed.

There are several additional clustering methods in use. Among those the gas aggregation technique has ardent adepts: Vapours from a heated crucible are mixed into a cooled noble gas flow where they nucleate and grow clusters[45]. Many interesting first observations in the cluster field have been obtained with this source[46].

Another aggregation technique is a variant of *Timms*'s «atomic vapour synthesis» machine[47]: Atomic metal vapour is cocondensed with a noble gas onto a target usually < 10 K. Then the matrix is slowly heated by radiation which leads to the diffusion of atoms out of their cages. When they meet aggregation may ensue. It is difficult to control this process. The particles formed have first been analyzed by UV/VIS absorption spectroscopy. This has, however, not been very successful because beyond the dimer the superimposed spectra from unknown particle concentrations with unknown absorptions could not be sorted out. The observation is, of course, not particle specific[48]. In contrast, spectacular success was obtained with Raman- and especially ESR-spectroscopy for M_3 up to M_7[40b]. The odd numbered alkali metal clusters from Li, Na, and K have given the first structure determinations available today apart from the predictions based on electronic structure calculations (and electronic spectra of M_3 in the gas phase), to be discussed in Section 4.

4. Proof of the Molecular Nature of Small Metal Clusters

It may be overcautious to prove that there is nothing mysterious with small metal clusters beyond what chemistry and quantum chemistry have taught us about the nature of molecules. It is true that we have problems writing a Lewis electron pair formula for a perfectly stable particle like Na_3 (!) or Na_4. However, we would not expect this to work anyway since these molecules are even more electron deficient than boron hydrides which also do not obey *G.N. Lewis*. Furthermore, these clusters cannot be bottled and sold and so don't belong to the category of commercializable stability for whose prediction the simple rules of chemical valency were originally invented[49]. Quantum chemistry has long transcended chemical bonding paradigms beyond the commonplace zeroth order models. Here is what one finds for the smaller clusters:

4.1. Dimers

All possible 15 homo- and heteronuclear alkali metal dimers are (essentially) Lewis-type electron pair bonded systems with a $^1\Sigma_g^+$ ground state giving a dissociation

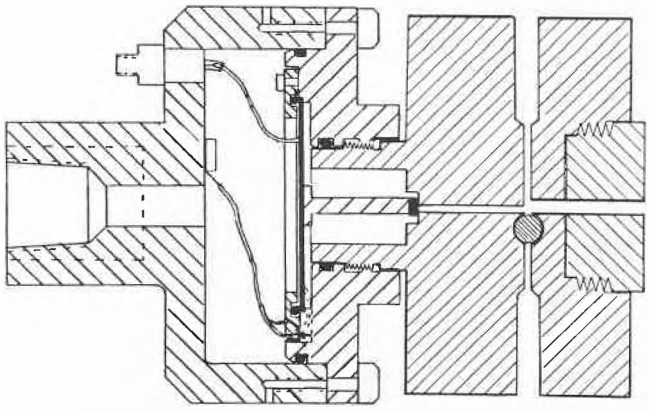

Fig. 4. Laser pulse evaporation source used for refractory metals with boiling point $\geqslant 2000\,^\circ C$. In the right metal block we see the cross section of the round target rod which is slowly turned in a spiral motion. Vertical to it is the entry tube for the laser light to be focused on to that rod. The horizontal tube is blocked to the left by the pulsed valve which admits He at 3 atm from the left. To the right is the opening towards the vacuum system. During operation a gas pulse is generated by opening the valve for 0.1 ms, then the laser pulse evaporates a metal plasma into the gas flow which is rapidly quenched, nucleates, and grows clusters which are expelled at the right nozzle opening. Scale of the source ≈ 5 cm diameter. Special embodiments of the exit tube allow to attach a fast flow reactor to study microheterogeneous catalysis in the gas without the necessity to put the clusters on a surface. Pt clusters formed by this tool can be collected on Al_2O_3 ceramics. They have shown hydrogenation activity more than 5000 times per Pt atom in comparison with the best industrial catalysts [106].

energy $D_0 = 1.06$ (Li_2)–0.45 (Cs_2) eV similar to H_2 (but $D_0 = 4.4$ eV!). The electronic spectra are also hydrogen-like. In Fig. 5 the first seven states of LiNa[50] are shown.

State-of-the-art *ab initio* quantum chemistry by *Meyer* et al.[51] has produced Morse- (Klein, Rydberg, Rees or Dunham-) parameters for all dimers up to K_2 which predict the experimental data to within ≈ 1 cm^{-1} (where this unit is applicable): In addition to the ground state the term energies and ionization potentials of more than ten excited singlet and triplet states and their D_e, B_e, ω_e, $\omega_e x_e$, α_e, r_e constants, dipole moments for the heteronuclear dimers, spin densities, spin-orbit coupling constants, lifetimes of excited states, line-widths of spectral transitions, and other properties (like perturbed states by predissociation, avoided curve crossings, different *Hund*'s coupling cases) are calculated to experimental accuracy. Sometimes *Meyer* tells the spectroscopists where they have made observational errors! However, this excellent agreement was only possible to achieve by explicitely treating the core electrons using an effective core polarization potential in an all-electron SCF/valence calculation including core-valence electron correlation. Any valence electron only calculation fails to account for even the crudest estimation of the properties of these dimers. The influence of the core-valence electron interaction is a (trivial but) not easily treatable difference between the alkali metal dimers and hydrogen. One consequence of it is the fact, that the «one-electron» bond in the homonuclear and in some but not all heteronuclear dimer cations is stronger than the electron pair bond of the neutral dimer[52]. Hence, the paradigm that a pair bond is about twice as strong as a (formal) one-electron bond, which is one of the fallacies learned by every chemistry student, is exactly true for hydrogen only! A second, more subtle, difference is obviously that the alkali metal dimers condense exoergically to a body-centered cubic (bcc) metal, if allowed to do so, while hydrogen molecules are not forming a metal even at the highest pressures probed so far (≈ 5 Mbar)[53] (for modelling Jupiter's core metallic hydrogen is assumed). The main property to consider for this difference is the large 1s-(2s)2p gap of 10.2 eV in the H-atom compared to the much smaller ns-np gap in the alkali metal atoms, 1.9 eV for Li and less for the others. A spectroscopic pearl has been found in LiNa (already known from H_2 and recently observed in Li_2): Through interaction with the heterolytic final state $Na^{\oplus}Li^{\ominus}$ ion pair the neutral D-state shows a double minimum potential as seen in Fig. 5 with two quite different vibrational progressions.

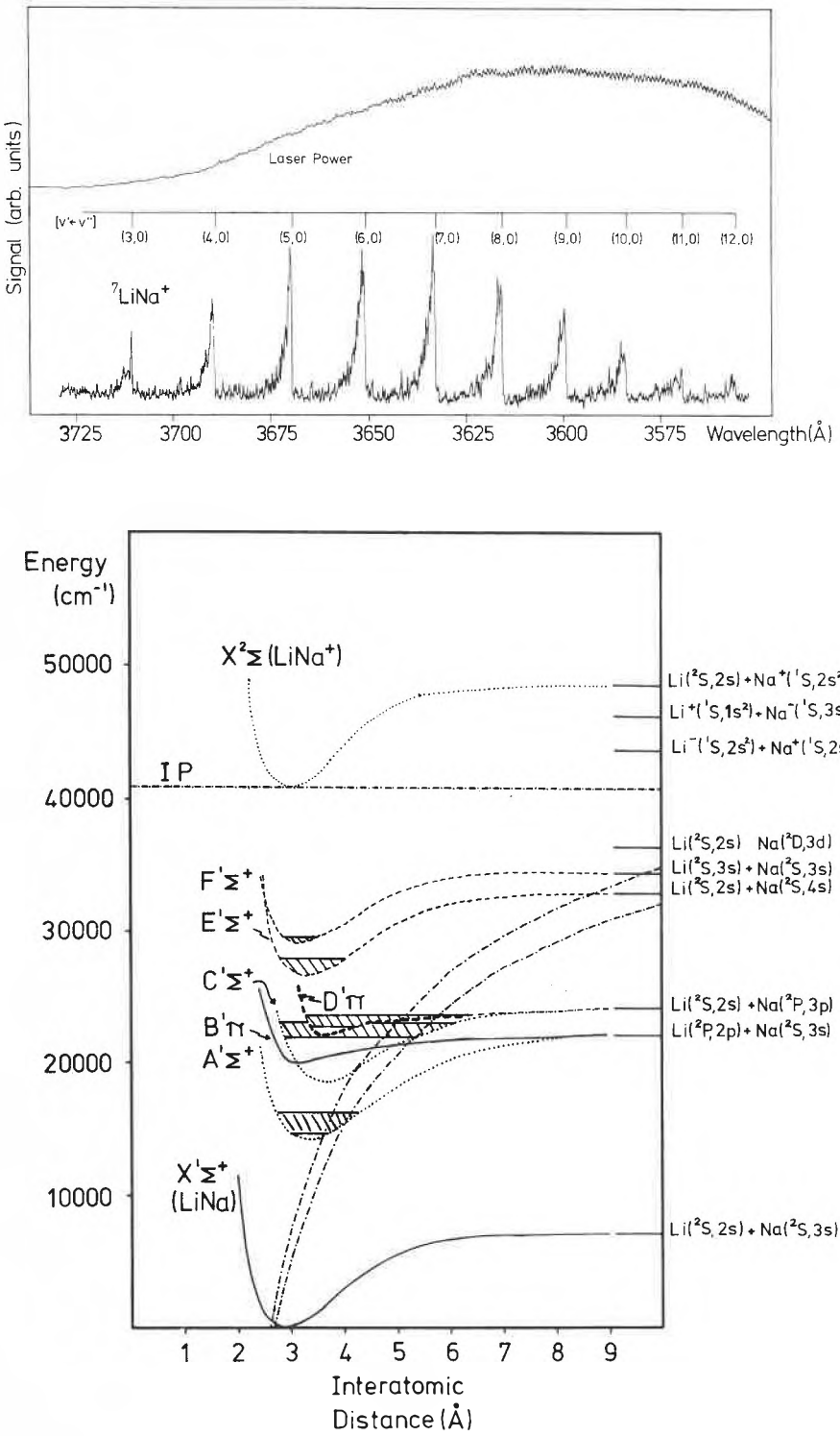

Fig. 5. Upper part: LiNa spectrum of the electronic E←X transition showing a vibrational progression with partially resolved rotation measured in a molecular beam with many species Li_xNa_y; particle specificity has been achieved by the two-colour, two-photon, one-photon resonant photoionization scheme as proposed and realized in Ref.[28]*. The signal has been measured with a quadrupole mass filter. The spectrum is uncorrected for the wavelength-dependent laser power shown on top. – Lower part: The newly discovered electronic states of this interesting dimer. Note state D which shows a double minimum potential*[50].

In summary: *Alkali metal dimers* are now well known and understood molecules. Especially Na_2 is in some respects even better investigated than H_2 and has become, therefore, a prototype for a covalently bonded molecule. Its properties have a wider scope for generalization than those of H_2, because the constituent atoms have a core like all other elements except hydrogen. – *Alkaline earth metal dimers* are essentially non-bonded van der Waals aggregates, $D_0 \approx 0.1$–0.2 eV, with a superficial analogy to the unstable He_2[54].

Transition metal dimers: In jumping to the 3d transition metal dimers the first example with d-electrons is Sc_2 formed from two ($3d4s^2$) ^{2}D atoms with $D_0 = 1.13 \pm 0.2$ eV[55]. It appears that its ground state is a $^5\Sigma_u^-$ state[56] which does not correlate with a dissociation limit of two ^{2}D atoms, however. Hence, its forma-

tion induces s-d excitation and spin reorganization. After Ti_2 with $D_0 = 1.3$ eV and (probably) $^1\Sigma_g^+$ and a stability optimum of $D_0 = 2.5$ eV with $^3\Sigma_g^-$ V_2, bond energy falls to $D_0 = 1.6$ eV with Cr_2 from two $(3d^54s)^7S$ atoms. *Cotton* predicted a hexupel bonded $(d_{z^2}\sigma^2 d_{xz}\pi^2 d_{yz}\pi^2 d_{xy}\delta^2 d_{x^2-y^2}\delta^2 s\sigma^2)$ $^1\Sigma_g^+$ ground state. This is consistent with some of the experimental information but not with the comparatively low stability which should be higher than that of V_2. The quantum chemistry[57] of this molecule proved to be a nightmare. After several abortive attempts with the generalized VB-method which only gave van der Waals molecules, the pseudopotential local spin density functional formalism came up with a satisfactory explanation of the experimental data[58]. As a consequence it became clear that *Cotton*'s qualitative description of a hexuple bond is not entirely correct since it is not able to link the dissociation of the molecule to two ground-state Cr atoms. Above Cr there are more electrons than accessible bonding orbitals in axial symmetry can accommodate so filling of non- or anti-bonding orbitals leads to «lone pairs». However, the dominant change in comparison to Sc–Cr is the drop-out of the d-electrons from effective bonding which they manifest in the first four dimers. Mn_2 $(3d^54s^2)^6S$ surprisingly is only a van der Waals molecule with a $^1\Sigma_g^+$ ground state of $D_0 = 0.23$ eV as if the two $4s^2$ atom shells were essentially alone. The half-filled d-shell $3d^5$ of both atoms decide to rest in weak antiferromagnetic coupling (i.e. form ↓ and ↑ spin non-bonding pairs) with a coupling constant of only 9 ± 3 cm^{-1}. Fe_2 has a $^7\Delta_u$ ground state with 6 unpaired electrons and a single s-s σ bond of $D_0 = 1.04$ eV. However, within an energy range of 0.5 eV of the ground state there are no less than 112 electronic states all arising from the interaction of two $3d^74s^1$ atoms formed by promotion from the atom ground state $3d^64s^2$ [59]. They all have slightly different Dunham parameters and thus produce a hopelessly complex absorption spectrum. This is the price to pay for not giving Fe_2 decent clothing as in $Fe_2(CO)_9$ or $[(CO)_4Fe{-}Fe(CO_4)]^{2\ominus}$.

One can now see why we have, at present, to stay with simple elements like alkali metals for serious physical chemistry on bare clusters. Co_2 ($D_0 = 1.7$ eV) and Ni_2 ($D_0 = 2.7$ eV) are similarly complicated and no agreement exists even for the assignment of the ground state. Note, that the homonuclear 3d dimer energies form the usual double hump with a minimum at Mn known from so many facts of 3d-TM chemistry. Ni_2 is the most stable dimer.

Advancing to the group 1b (11) dimers Cu_2, Ag_2, Au_2, and their heteronuclear combinations, we have (superficially) alkali metal dimer like single bonded molecules which behave innocently. In the course of traversing the nd transition row the d-orbitals contract so much that they are now housing nearly non-bonding core electrons. D_0 values are 2.03, 1.69, and 2.29 eV for the dimers of Cu, Ag, and Au, respectively. The detailed quantum chemistry of Cu_2 involved configuration interaction amongst all 22 $3d^{10}4s^1$ electrons[60] and is thus even more expensive than treating the alkali metal dimers together with their core electrons. Zn, Cd, and Hg only form weak van der Waals dimers like group 2 metals with $D_0 = 0.2$, 0.087, 0.06 eV, respectively.

We concentrate on those dimers which play a role in the larger clusters to be viewed in Section 5. Many more of the 4272 dimers of 92 elements or of the 2145 of metallic elements are known today.

4.2. *Trimers*

Common nomenclature attributes the term «cluster» from the trimer on up. Hence, making and understanding M_3 was an essential first step in cluster science. All alkali metals – to start again with these prototypal metallic elements – give stable trimers, very stable trimer cations, and less stable trimer anions. Li_3 has an atomization enthalpy of 174 ± 15 kJ/mol[19] or 58 kJ/mol per atom as compared to 51.4 kJ/mol per atom in Li_2 or 155.2 kJ/mol for bulk Li-metal. Even higher stabilities have been measured for the group 1b (11) trimers whose theory is remarkably similar.

Comparison to H_3: It is common knowledge that the original «lake Eyring»[61], the H_3 site on the potential energy surface of three hydrogen atoms has long dried up completely: H_3 is unstable in the ground state and represents a ridge not an intermediate on the reaction path $H_2 + H$. Why then are the alkali metal trimers stable? A lucid semi-empirical argument by *Calzaferri*[62] shows, that it is again the small ns-np gap of the alkali metal atoms in comparison to the unsurmountable 1s-(2s)2p gap of H that is decisive. Participation of p-orbitals is essential for the third alkali metal atom to stick to the previously formed dimer. Only in excited states of H_3^*, where a strong admixture of the 2p level takes place, does one also obtain stability as shown by *Herzberg*[63] for H_3 in high Rydberg states.

Spectroscopy of Na_3: It was a challenge to measure the absorption spectrum of Na_3 for the first time. The MS signal at m/z 69 was observed using a two-stage photoionization scheme: One laser photon with tunable colour was used to populate a neutral excited state, while a second, fixed colour laser photon was promoting the excited state population into the detectable ion state. Thus the m/z 69 intensity should vary with the transition probability as a function of laser frequency and hence map out the spectrum as had previously been shown for the first time with Na_2[64]. Not before *Scholl*[65] had predicted the position of the first few absorption bands by an SCF-XαSW calculation were we able to locate two bands of the Na_3 spectrum in the red part of the visible at 665 (sharp A band) and 625 nm (long virbrational progression B band)[66]. Since then two or three more bands B′, C, and D, have been found which were not observable with cw-lasers but easily seen with pulsed laser excitation because of the short lifetimes of the neutral excited states[67]. *Wöste* and his students at the EPF Lausanne have remeasured the Na_3 A, B band spectrum whose discovery he has coauthored with *Herrmann* and *Leutwyler* when he was my doctorand. This time a much colder beam (< 10 K for the dimer, probably about 20 K for the trimer vibration) and a more sensitive molecular beam machine were available. Both helped to obtain highly resolved A and B bands which allowed a detailed analysis to which many people have contributed[67].

Na_3, the first totally investigated Jahn-Teller molecule:

Let us summarize a long and fascinating story which several years ago has been enriched by measuring the spectra of Li_2Na, $LiNa_2$[68] and recently by a first glimpse at Li_3[69]. We stress the physical concepts involved without going into mathematical details (see Ref.[71] for these): In the heteronuclear Li_2Na, and similarly in $LiNa_2$, Na_2K, NaK_2 etc. the isomers LiLiNa and LiNaLi or even ^{6}LiNa^{7}Li, ^{6}Li^{7}LiNa, ^{7}Li^{6}LiNa are indistinguishable. This suggests a ring structure and in the homonuclear case Li_3 and Na_3 equivalence of the three atoms, hence an equilateral triangle. However, the ESR spectrum of Na_3 frozen in an argon matrix below 10 K as first measured by *Lindsay* et al.[40b] was only interpretable with C_{2v} symmetry: High spin density at the base atoms of a (probably) obtuse isosceles triangle with very low spin density at the apex was found. But on slowly heating the matrix the ESR spectrum became confused and reached a new sharp pattern above 25 K where the three atoms assumed (statistical) equivalence, hence D_{3h} symmetry. What happened has meanwhile been clarified to the extent that it has become the schoolbook case of *Jahn-Teller* (JT) *instability*. If these trimers are not linear but assume a ring structure as suggested by the isotope substitution experiments then they would have a degenerate electronic ground state $^2E'$ in D_{3h} symmetry. This violates the fundamental requirement of quantum mechanics for a single valued solution of the Schrödinger equation and is caused by the assumption of separability of the electronic and nuclear motions, as stated in the Born-Oppenheimer theorem. Coupling of this electronic state with the degenerate normal coordinate vibration e′ to form vibronic, the coupled vibrational-electronic states $E' \times e'$, lifts the degeneracy leading for Li_3 to a potential surface first calculated by *Gerber*[70] and shown in Fig. 6 (similar surfaces have been computed for all the alkali metal trimers, see references in[78]).

The general theory of these phenomena has long ago been established by *Longuet-*

Higgins and others[71]. For non-totally symmetric displacements of the nuclei we obtain a splitting of the degenerate electronic states into two species of C_{2v} symmetry with different energies and vibrational constants. Their lower and higher potential surfaces E_- and E_+ intersect in a point on the C_3 axis of the figure where we still have degeneracy. The vibronic ground state E_- has a lower energy than the avoided Born-Oppenheimer pure electronic state E'. The difference is called Jahn-Teller stabilization (a virtual stabilization, because the reference state simply does not exist!). Only the E_- surface is shown in Fig. 6 for the ground and an excited state. The coordinates are the vibrational displacement vectors of the two components of the degenerate e′ normal coordinate causing the splitting (a bending type motion and an asymmetric stretch; the first together with the totally symmetric, non-degenerate vibration is shown at top left in Fig. 9). Hence Fig. 6 does *not* represent a real space energy surface but a normal coordinate space surface. The threefold symmetry is invariant but the equilateral triangular centre is now a cusp – the crossing point of the E_- and E_+ surface – and not a well. Instead there are three equivalent wells marking three conformers with equivalent isosceles triangles generated by a cyclic permutation of the role of the apex atom. Actual physical permutation requires an oscillation of the molecule from obtuse to acute angled C_{2v} and back thrice for one permutation cycle, never passing through the D_{3h} centre. This is equivalent for the representative masspoint to go once around the «moat» in Fig. 6 even though none of the atoms actually leaves its hole in real space. If the energy barrier between the wells is small enough compared to kT this permutation leads to an actual hindered or (quasi)free physical rotatory motion of every atom *in its proper well* called *pseudorotation*. This is linked to the *vibrational angular momentum* of a superposition of the two normal coordinate components in the e′ mode as shown in Fig. 7. It adds a component to the total angular momentum around the C_3 axis which is the true signature of a *dynamic* JT effect or of a *floppy* molecule that can be observed in the free gaseous state.

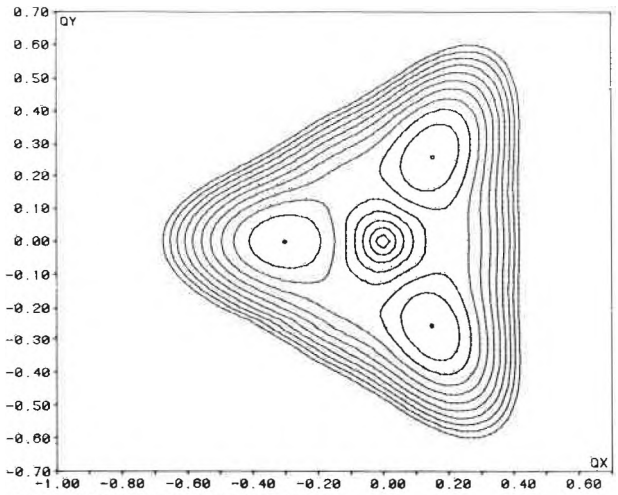

Fig. 6. Cross section of the potential energy surface E_- of Li_3 in the coordinates Q_x/Q_y, the displacement coordinates for the two components of the doubly degenerate e′ vibration in D_{3h} symmetry[70]*. Lower part: ground state; upper part: E″ excited state. The equidistance of the contours is 50 cm^{-1}. Note the central cusp in the lower part which goes up and joins the E_+ surface in the [0,0] point. The location minima in the lower surface, marked by a point, are very shallow with Li_3. They form wells of more than 100 cm^{-1} depth in the excited state. The minima represent obtuse isosceles conformers while the barrier ridge between two minima is acute angled (obtuse and acute relate to the 60° angle of the equilateral triangle). The upper surface in Li_3 is very similar in qualitative aspects to the ground state surface in Na_3 (not shown).*

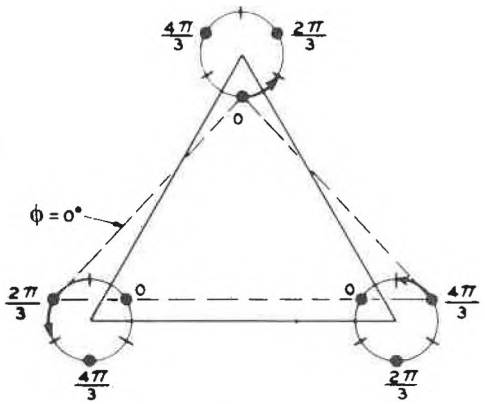

Fig. 7. Visualization of the pseudorotational movement of the three atoms in their wells caused by the thermally excited transformation of the three conformers. The dashed isosceles triangle is one extreme position of the vibration while the other, the acute triangle, is not shown but easily constructed by connecting the topmost vertical bar with the bars at 4 o'clock on the left and 8 o'clock on the right bottom atoms, respectively. The equilateral triangular situation would be the vibration-less equilibrium position of a non-JT-molecule, never reached in this case.

Before presenting spectral proof we can now already interpret the following observations: When pseudorotation is fully excited we would expect *average behaviour* of a D_{3h} molecule where no conformers are distinguished. This explains the observed isotope scrambling and the «high»-temperature ESR-signal. If kT is small or the well deep (lifting of the degeneracy by a *static* JT deformation) the molecule would be frozen in any one of the three C_{2v} wells as documented in the «low»-temperature ESR spectrum. Finally, if the experiment probes the molecules on a time scale short compared to the vibrational dislocation of the nuclei – i.e. an optical spectroscopic measurement in contrast to the «slow» ESR probe – we would always, i.e. independently of temperature, observe the molecule in one of the properly split Jahn-Teller wells of C_{2v} symmetry *and* in a defined pseudorotation quantum state (we do not want to enter the «structure controversy» at this point! Nobody has seen the free molecule in a statically deformed C_{2v} symmetry without pseudorotation (yet)).

This is exactly what the two-photon, two-colour, one-colour resonant ionization spectrum in the mass spectrometer shows (Fig. 8): The quantitative analysis of the B-band of Na_3[67], Fig. 8c, has verified this interpretation (see also Fig. 9 for an earlier assignment of the spectrum[70] which presents a cross section of the two absorption-coupled Jahn-Teller surfaces E_-, E_+). The well resolved structure in Fig. 8c allows to fit the progression to the formula predicted by theory for large Jahn-Teller distortion, to first approximation:

$$E(u,j) = (u + 1/2)\omega_0 + A\,j^2 \qquad (1)$$

where $u = 0,1,2, \ldots$ quantum number of a radial oscillator describing the distortion ($\approx$ the motion of an apex atom from the obtuse to the acute angle limit);
$j = \pm 1/2, \pm 3/2, \ldots$ quantum number of the pseudorotation with $A = \hbar/2I$ and $I = \mu r_0^2$ the moment of inertia around the rotation axis, μ the reduced mass, r_0 the mean distance from the minimum of the well.

The fit gives $\omega_0 = 128\ cm^{-1}$ (as found[66]) and $A = 4\ cm^{-1}$. The splitting of the u-vibrations is a tunneling split between the three wells of 3–5 cm^{-1}. The total JT stabilization amounts to 1050 cm^{-1} and the localization in the wells to 26 cm^{-1}. This has been deduced from a variational solution of the vibronic eigenvalue problem using 600 basis functions. A linear vibronic coupling constant of $k = 4.04$ and a small quadratic correction of $g = 0.012$ describe the spectrum to experimental precision[67]. Note the broadening of the pseudorotation «lines» with increasing j. This is the mark of 1) a weakening of the first order approximation which is strictly valid for cylindrical deformation only and will work less for larger pseudorotational amplitudes; 2) of the non resolved proper rotation of the molecule (everyone of the pseudorotation «lines» is the envelope of a proper rotation band); 3) the (neglected) complications of electronic orbital and spin angular momentum. The other bands have not been interpreted to equal detail. The A-band is still best analyzed in *Radi*'s thesis[68], and a band equivalent to the B-band, but of course not JT-influenced, has been analyzed for the Li_2Na and $LiNa_2$ molecules[68].

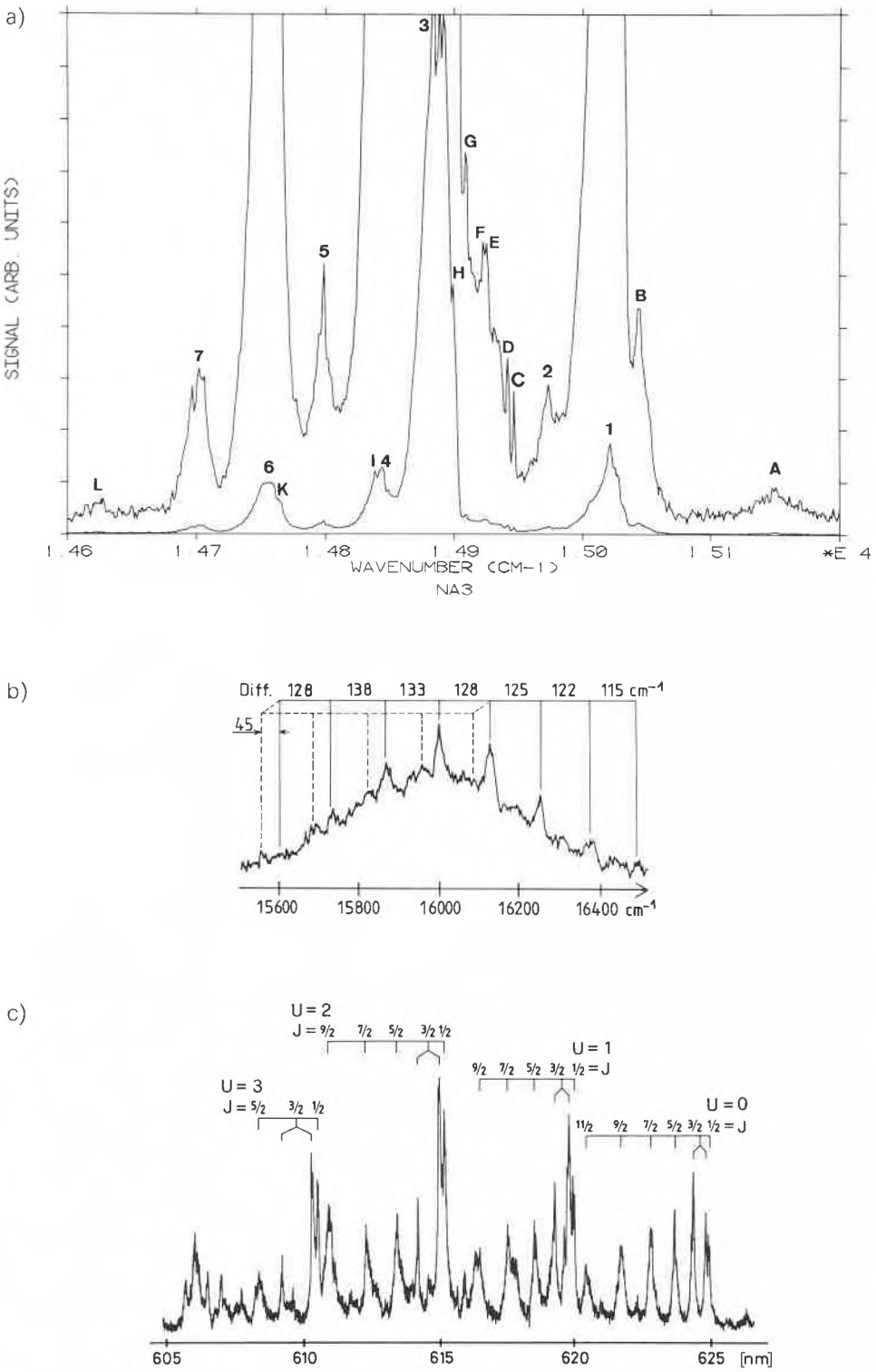

Fig. 8. a) A-Band of Na_3[66,68], b) B-band[66,68], and finally c) the much better resolved B-band by Wöste et al.[67]. *Note the half-integer pseudorotational progressions, the mark of the dynamical Jahn-Teller effect, to be explained in the text.*

«Fractional quantum numbers»:

The half-integer quantum number is the signature of pseudorotation. As already pointed out by *Longuet-Higgins*[72], going once around the «moat» in Fig. 6, i.e. a rotation by 2π around the C_3 axis, leaves the vibronic wave functions with reversed sign, hence the full rotation is not an identity operation of the vibronic system. Going twice around rectifies this deficiency (similar to the necessity to introduce double groups with half integer J, well-known in transition metal chemistry). Since rotation by 4π is an identity operation the rotational quantum numbers, which are based on the normal 2π rotational identity, become half integers (the term «fractional» quantum number as used by *Delacrétaz* et al.[67] is a cautious hint at the underlying approximation. If the deformation is not strictly cylindrical, i.e. $k \gg g$, the j defined in Equation (1) is not any longer a good quantum number and deviates from exact half integers).

Half integers for the j-quantum number advertise pseudorotation. In solid matrices rotation is quenched, hence (quasi)free pseudorotation has not been observed. This explains why it is very difficult or impossible to understand the Jahn-Teller «effect» quantitatively in solids. One has to use a gaseous molecule to carry experiment and theory to a good end as has been shown for Na_3[67,70]. – The difference between the measured Na_3 and the reproduced Li_3 case is a much lower pseudorotation barrier in Li_3, hence it has not been possible to freeze out C_{2v} Li_3. The same is

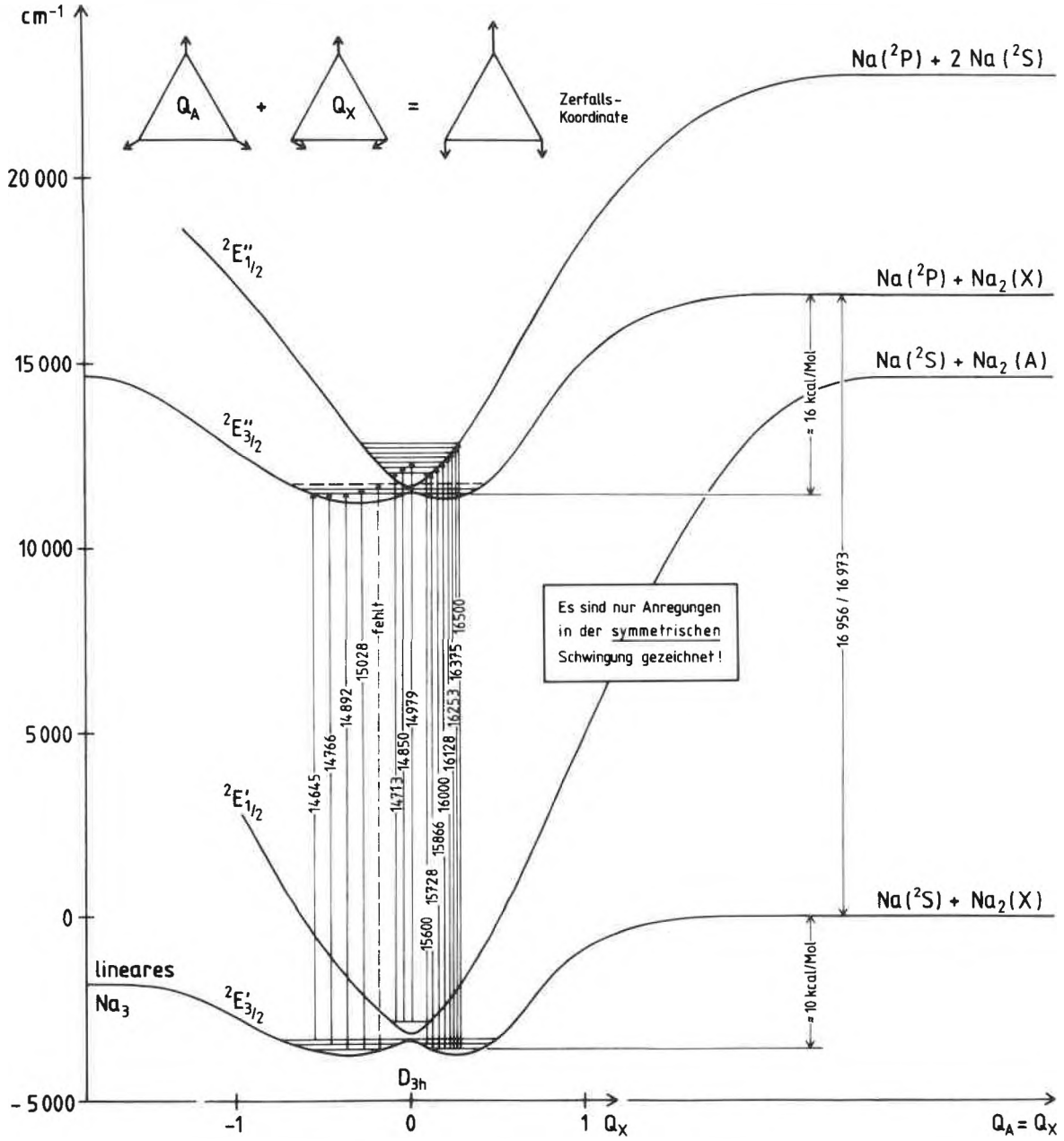

Fig. 9. Proposal for the interpretation of the Na_3 spectrum (A, B-bands) by Gerber [70]. The quantitative energy terms have been obtained by proper scaling of several Na_3/Na_2 properties by those of Li_3/Li_2 both from experimental and calculated data. Cross sections through the D_{3h} point with Q_x and Q_A, defined at top left, as abscissa, are shown. The lower E_- and the higher E_+ Jahn-Teller surfaces of the ground E′ and the excited E″ states are drawn. The dissociation channels to ground or excited state atoms and dimers are on the right. Several observed transitions [66] are assigned with arrows. The large amplitude distortion to a triatomic linear molecule is discernible to the left.

true for Cu_3. A recent theoretical study[73] shows the E_- surface of the ground state of Na_3. It looks qualitatively similar to the excited state surface of Li_3 in Fig. 6. This paper also claims that the B-state of Na_3 may be even more complex than believed. It appears to be a mixture of the degenerate E′ state with the A_1' state in which the coupling between the different states is stronger than that of the E′ components. Experimental verification of this prediction does not exist presently.

Magnetism of M_3:

What influence has the odd spin on these doublet molecules? There are four components of angular momentum around the C_3 axis: the proper rotation, the vibronic part generated by the superposition of the two components of the e′ mode (with 90° phase shift) or pseudorotation, and the electronic spin and orbital contributions. The E′ state has only σ character, hence no orbital angular momentum. But the main spectral transition is a $\pi^* \leftarrow \sigma$ like $^2E'' \leftarrow {}^2E'$ excitation whose upper state has an orbital angular momentum which «contaminates» the spectrum. Only this four component angular momentum vector has a «good» quantum number (represents a constant of motion of the system) independent of the strength of vibronic coupling and Jahn-Teller splitting. Inclusion of spin removes the crossing point of the lower and higher Jahn-Teller surfaces at the cusp (see Fig. 9).

An interesting consequence of the coupling of the four components of angular momentum, especially the spin-rotation coupling, is found when magnetic deflection of the beam is probed with a Stern-Gerlach magnet (Na_3[74], several alkali metal trimers[75]). Naively one would expect Na_3 to show 1/3rd of the deflection of the Na atom when it moves at the same speed through the same inhomogeneous field: The force pivots on the same spin moment of 1/2 $\hbar$, but the ratio of the masses is 3:1. Instead a distribution curve is observed which has the largest intensity at zero deflection – as if the majority of particles were nonmagnetic – fanning out to a smaller local intensity maximum (if at all) at the expected value of 1/3 of the atom. With increasing temperature higher rotational states are populated decreasing the signal at 1/3 deflection even more.

With higher deflecting fields more intensity arrives at 1/3. It has been derived by *Gerber* [76] that only that part of the magnetic moment is effective for the deflection which is projected out from the combined spin-rotation vector onto the magnetic field gradient. Since the total angular momentum projection has to obey the rules of quantum mechanics the higher the rotational quantum number the smaller is the effective magnetic moment of the spin component if this cannot be decoupled from rotation by a strong field. If all this is properly computed using the actual rotational state population, considering symmetry constraints for the trajectories of the precessing molecule, and the JT-imposed pseudorotation, the experimental distribution can be reproduced. It is then possible to gain the value of the magnetic moment by virtue of the known theory of the distribution curve.

Let us stop here with details known on M_3 whose wealth we have only gleaned superficially. The exposure to it had as motive the proof that no further components are necessary to its understanding than those established by molecular science. In fact, the electron density plots and even the spectroscopic details are qualitatively not different from those of the cyclopropenyl radical or even of the 1,3,5-trifluorobenzene cation [77], a perfect Jahn-Teller molecule.

Beyond M_3 information is drastically dwindling.

4.3. Polymers

Fig. 10 shows the calculated structures of Li_x clusters up to $x = 10$ as obtained with a multireference SCF/CI *ab initio* method by *Koutecký* and his colleagues [78]. The quality of these calculations belongs to the best of what is possible today. In fact, where data exist – ESR measurements of Li_3, Li_5, Li_7; enthalpies of Li_2 to Li_4; ionization potentials of the whole series; qualitative stability arguments derived from mass spectrometric intensities (see Section 6) – very good predictions of the experimental quantities have been given. It is to be understood that the structures have been obtained by a minimum search of the Hellmann-Feynman forces (which vanish at every minimum of the potential hypersurface). Starting statistically from many different non-equilibrium structures the best minimum found is most likely the preferred stable conformation of the system. That is shown in Fig. 10. One slight reservation is in order: The conformations are valid for the R_e structure only, i.e. at 0 K without any zero point vibration. Since many of these particles show Jahn-Teller instability similar to Li_3 with only small pseudorotation barriers the average structure obtained at finite temperatures (as it would be probed by an X-ray experiment) might often be of higher symmetry than what is seen in Fig. 10. We leave the contemplation of the bizarre and unexpected shapes to the reader. He is probably most shocked by the long prevalence of flat structures since the first 3-dimensional shape occurs with Li_7. Intuition would not connect the undirected metal bond with such rafts. In fact macroscopic metal structures are typical for their compact, closest packed arrangement of atoms. Why should small clusters be so open? This is also a fundamental difference between free and ligand-covered clusters.

Simple HMO arguments:

We see the main reason already with Li_4. This electron deficient system would have to form 6 bonds spanned by $a_1^2t_2^2$ in T_d symmetry creating a Jahn-Teller unstable tetrahedron. Its disphenoidal deformation to C_{2v} is sufficient to lift the degeneracy but a simple HMO argument shows why the flat rhombus or lozenge with D_{2h} symmetry is the most stable, closed shell structure: Construct the topological matrix for a tetrahedron with atoms numbered 1 to 4. Introduce variable β parameters for the atom 1–2 and 3–4 interactions leaving the rest unchanged. Now let β_{12} go to zero, breaking the 1–2 bond. This will lower the energy and end at a minimum with $\beta_{13} = \beta_{14} = \beta_{23} = \beta_{24} < \beta_{34}$ representing a flat rhombus. Of course, $\{LiCH_3\}$ has a nice metal cluster complex structure with tetrahedral units $(CH_3Li)_4$, i.e. a Li_4-cluster with a methyl group on the centre of every face [79]. Here we have electron saturation with the noble gas shell $a_1^2t_2^6$ and hence no objection to a tetrahedral arrangement (note that we do not obtain Lewis electron pair bonds, but multicentre bonds have been accepted long ago). This sort of argument can be made for all the rest of the bizarre structures. For an inorganic chemist trained in high-symmetry coordination chemistry where zeroth order ligand field arguments work so well, the raft of Li_6 is a criminal offence. He would prefer the octahedron. However, 6 electrons are not

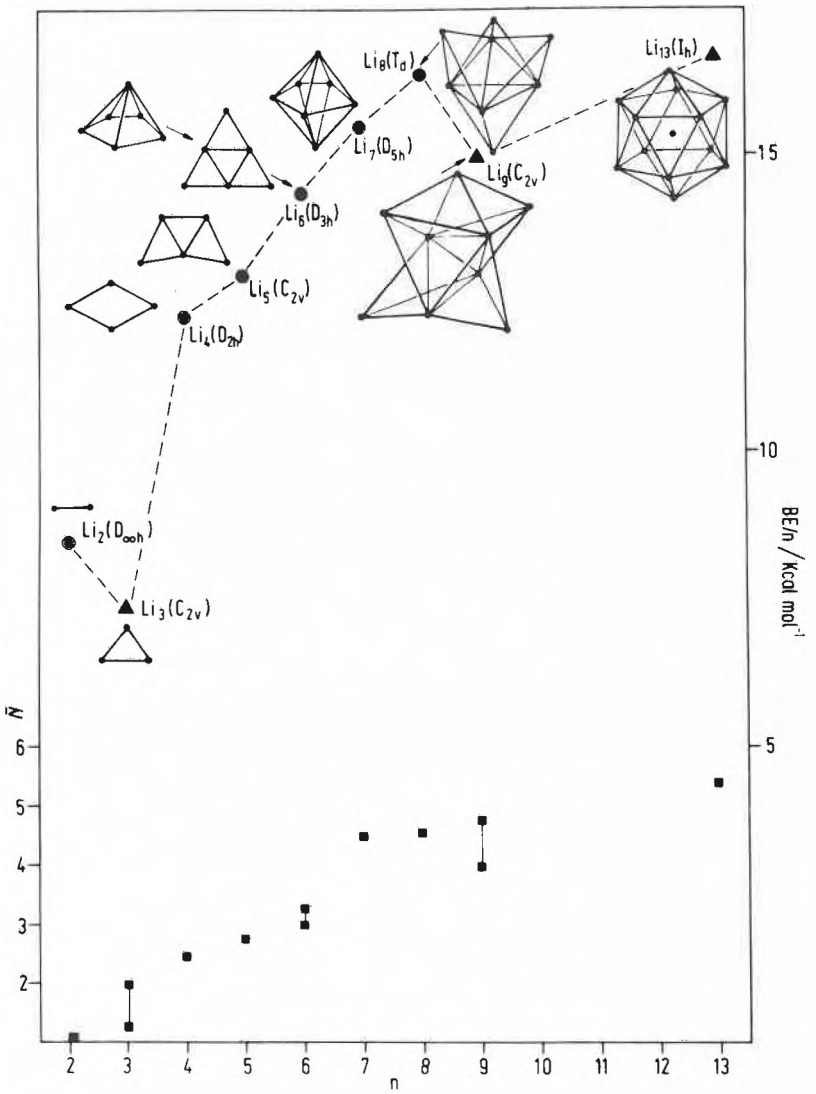

Fig. 10. Structure and bonding energy of Li_x clusters as computed with an MC-SCF-CI method by Koutecký et al. [78]. Note the 2-dimensional forms prevailing up to $x = 6$, explained in the text. After reaching Li_8 with a structure similar to $Li_4(CH_3)_4$ [79], a drop in bond energy occurs towards Li_9. Although the body-centred icosahedron Li_{13} looks good it is unstable towards growth to larger clusters and hence not an abundant species in any free metal cluster family studied to date. It is of prominent stability with metal cluster complexes [22], however.

enough to make a closed shell system in the $a_{1g}^2 t_{1u}^4$ manifold. So a similar breakdown convinces him of the stability of the raft: Start with the topological matrix of an octahedron numbered 1,2,3 and 4,5,6 for two opposing trigonal faces and represent the 12 equivalent nearest-neighbour interactions with the same β. Sever the bonds 1–2, 2–3, and 1–3 by setting their $\beta = 0$. You end with a closed shell system of much lower energy having D_{3h} symmetry with the closed shell orbital occupations $(a_1')^2(e')^4$. Of course, these simplistic arguments have really to be replaced by the painstaking yet fascinating discussion in the papers of *Koutecký* et al. These have now advanced to M_{20}. For the larger clusters a less refined basis had to be used and present computational facilities, even on a Cray-II, do not make it feasible to go much beyond this size without sacrificing precision. Therefore, we expect to have only a slightly blurred view on larger systems and to put up with much coarser models of the physical system (cf. Sections 5 and 6).

Summary of Section 4:

The dimers and small clusters looked at so far do not show any property which could not be explained by the well established tools of molecular spectroscopy and electronic structure theory. MO-type methods use delocalized orbitals as a starting basis which, however, would show various degrees of localization in the most stable structures if looked at in detail. A renaissance of the VB method, the generalized valence bond (GVB) method, which starts with a very different basis has led to practically identical results where applicable (e.g. Ref. [73]).

We conclude that the bare metal-metal bonded clusters compensate for electronic unsaturation and threatening high multiplicity by lowering their symmetry in comparison to metal cluster complexes which choose the number of ligands such that they achieve an optimal electronic bonding complement in usually closed shell high symmetry configurations.

(This is, however, a much too sweeping statement to cover the rich cabinet of curiosities in the chemistry of transition metal cluster complexes.) We do not hesitate to admit that small metal clusters do fit nicely into the body of accumulated knowledge of molecular chemistry without the necessity to invent any new concept.

5. From Molecular Cluster to Bulk

We choose a simple property to go all the way from the atom passing molecular clusters with increasing sizes to finally reach the bulk: the *ionization potential, IP*. This probes, in the simplest case, the location of the highest occupied level in comparison to the vacuum level. In the bulk it is the well tabulated electronic *work function*. Since this depends on the Miller index of the electron emitting plane of a crystalline metal we take the «polycrystalline» work function usually measured at the pure liquid metal surface towards vacuum as representative of the bulk. The measurement of the *IP* of a cluster can be performed in the mass spectrometer, hence it is particle specific as mentioned in Section 3.

Ionization potentials by photoionization:

The usual sources for ionization of molecules in chemical mass spectroscopy are mostly inappropriate for our purpose. We use gentle photoionization instead. This gives very fine control of the energy of the ionizing photon if produced by a monochromator selecting a narrow range from a broad-band light source or by a tunable laser either pulsed or continuous. The experiment then consists of the following steps (not an actual run!): 1) choose the proper mass window on the MS, e.g. m/z 230 for observing $Na_{10}^{\oplus}$; 2) adjust the slit width of the monochromator to obtain an energy width of the photon of ±0.01 to ±0.04 eV; 3) begin at about 400 nm with zero ion current in the selected mass channel and scan slowly towards smaller wavelengths. Somewhere along the wavelength scale ions of m/z 230 start to appear if the precursor neutral is present in the molecular beam which is directed to pass through the middle of the ionization box of the ion source. Photoionization efficiency (PIE) curves similar to those shown for Na_2 to Na_{11} in Fig. 11 are then measured for every component of the beam one after the other. With a time-of-flight mass spectrometer (TOF) this measurement can be made simultaneously for all clusters present with one scan of wavelengths [80]. We usually choose the spectral width of the monochromator light such that the spectral resolution of the PIE-curve is not limited by that width but rather by the noise components present in the cluster ensemble itself (source not detector noise). There is no firm theoretical basis to date on how one has to extract a (vertical) ion-

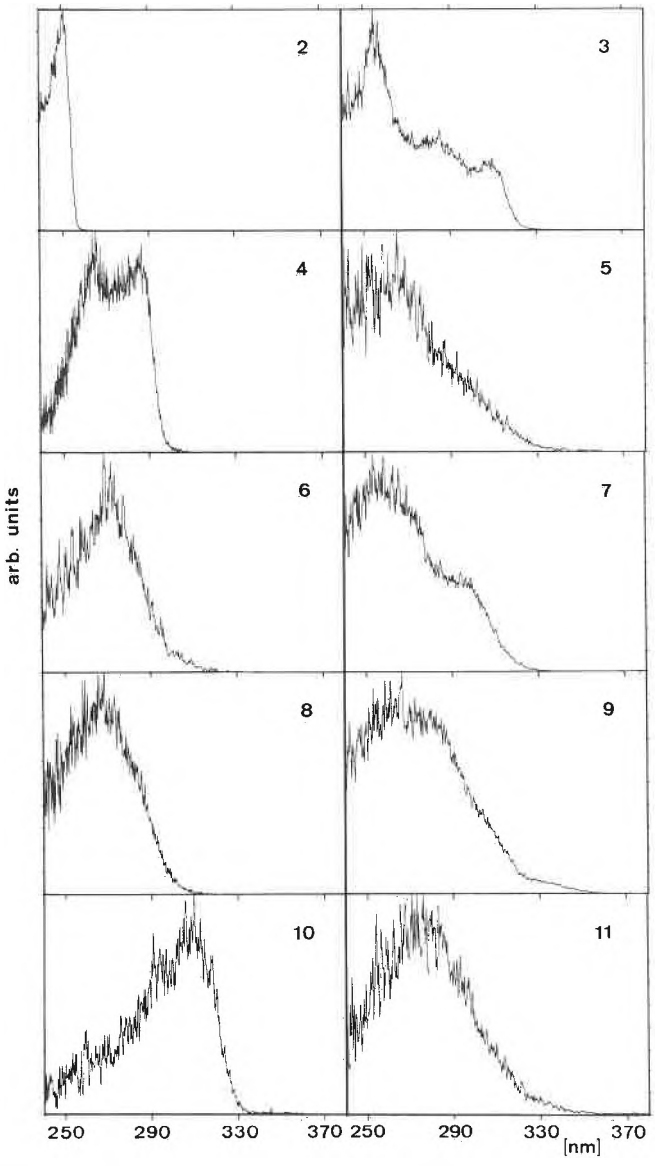

Fig. 11. Photoionization efficiency curves as directly measured for Na_2 to Na_{11} with a monochromator slit width equivalent to 0.01 eV. The long-wavelength tails to the right contain temperature information [33].

ization potential from a PIE-curve for a polyatomic molecule. However, there are several house recipes around which do not greatly vary from laboratory to laboratory so that we usually do not start fighting about them [81]. In Fig. 12 the *IP*'s from Na_2 to Na_{22} are shown [82], and in Fig. 13 we present the collected *IP*'s from the cluster families of several metals plotted in a special way to be understood as follows.

Model of the conductive droplet:

We introduce our first crude model. Suppose that these small clusters behave similarly to a conducting spherical droplet with size-invariant intrinsic properties as far as ionization is concerned. How does the ionization potential change if the radius of the droplet is monotonously increased and finally becomes arbitrarily large? Of course, an infinite radius means a flat surface of a metallic half-space. From this we know the ionization potential: It is the bulk work function. Now we want to describe the process of extracting an electron from this half-space in comparison to the process on a sphere with radius R. A simple argument in electrostatic image-charge theory [83] is quantitatively transparent: The Coulomb interaction of an electron with a flat metal surface at distance r can be described by the charge interaction of a positron sitting at $-r$ within the metal, so the force is $-e_0^2/4r^2$. When the electron moves farer away, the image charge does likewise in the opposite direction, and both finally vanish at $r \to \pm\infty$. With the finite sphere of radius R, the + image charge of the extracted electron at the distance r from the surface also sits in the metallic sphere somewhere between its surface and the centre. When the electron moves farer away the «positron» moves nearer to the centre and ends in the centre for total removal of the electron, because we have now again a spherically symmetric system of a singly charged positive ion. The total way of the positron is from R to 0, of the electron from $r = R$ to $r \to \infty$. Obviously the integral of the force over the distance r, the (potential) Coulomb energy, will be different in the flat and the curved case. Assuming that the energy of extraction of the electron from the «metallic electron sea» is independent of R one obtains:

$$IP(R) = W_{inf} + (3/8)e_0^2/R = W_{inf} + 5.40/R \text{ eV} \quad (2)$$

if R is measured in Ångstrøms, and where W_{inf} is the bulk work function (at $R \to \infty$). The *IP* of a spherical metallic droplet is size dependent in a simple way. $IP(R)$ plotted against $1/R$ should be a straight line with slope 5.4 eV·Å. How do we assign a radius R_n to a cluster of n atoms? The simplest way to do this is to take the atomic volume of the metal (atomic mass A/density ρ), divide it by N_a (Avogadro's constant) to obtain the volume of an atom, multiply it by n and assign a sphere to the same volume: $R_n \cong (3nA/4\pi\rho N_a)^{1/3}$. There

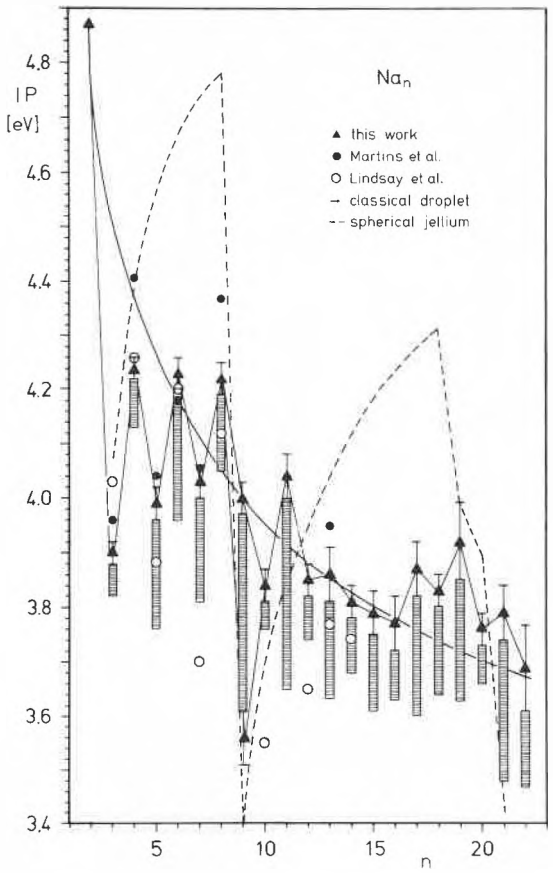

Fig. 12. Photoionization potentials for Na_2 to Na_{22} as derived from measurements similar to those shown in Fig. 11. The error bars contain the apparatus precision and uncertainty about the model for the extraction of the IP. The smooth curve is predicted by the classical conductive droplet model (Fig. 13), the dashed curve by the self-consistent spherical jellium mean field model (see text in Section 6). Filled circles mark the theoretical predictions by Martins, Car, and Buttet [92], using a local spin density approximation. Open circles give Lindsay's predictions from a parametrized HMO model. Note the pronounced odd-even variations in the IP's, whereby odd IP's < even IP's up to 9; from n = 10 it is reversed. The shaded vertical tails are an indication of the variable thermal pre-threshold tail. The longer it is the higher the cluster temperature (among other influences).

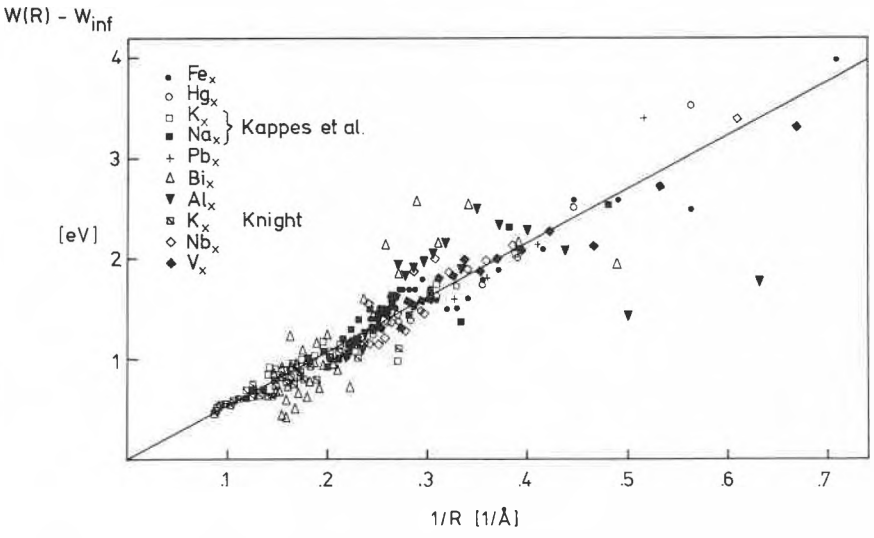

Fig. 13. Photoionization potentials of 10 different families of metal clusters from the atom to about M_{60} each. We plot the difference $IP(R) - W_{inf}$ where W_{inf} is the work function of the macroscopic metal against $1/R$ with R being equal to the radius of a sphere with the volume of n atoms for the M_n cluster. The straight line is not a fit. It is the size-dependent part of the ionization potential of a conductive droplet which has no specific parameters for a certain metal (see text). The convergence of the data to that line demonstrates that larger clusters assume gradually bulk properties and reach the bulk smoothly. This is true for most metals. Atoms with a closed valence shell show an abrupt drop of the IP, indicative of an insulator to metal transition occurring in a size range from 20–50 atoms as found with Hg [84].

are more refined ways to do this[80b], e.g. include surface tension and compressibility corrections, but the changes are minimal and not even well justified. Fig. 13 shows the result of such a plot. The ordinate $IP(R) - W_{inf}$ has been chosen to obtain the same starting point for all metals, and the straight line is not a fit but the universal formula (2). Since the plot starts with the atom for the 10 metals shown the scatter at the high $1/R$ end is easily understandable. Why should an atom behave as a liquid metal droplet! The same is true for the small molecular clusters. However, we see a nice convergence towards the model line at a cluster size of a few dozen atoms. The only large scatterer is Bi_x which under close scrutiny reveals to be a van der Waals adduct of Bi_4 molecules. There is one arbitrary adjustment in this plot which we have to correct immediately: For the *IP*'s of Hg_n clusters $1 \leq n \leq 11$ we had to subtract $W_{inf} + 2.44$ eV to get convergence to the zero ordinate. A year ago, *Hensel* et al.[84] were able to measure *IP*'s up to Hg_{40}. It turned out that between about Hg_{20} and Hg_{40} the *IP*'s fall smoothly by a total of 2.4 eV and now extrapolate in conformity with the model to the bulk work function. A similar plot can be made for the negative cluster ions, where $W_{inf} - EA(R)$ according to the model gives a straight line with $-(5/8)e_0^2/R$ and EA = electron affinity (see Ref.[25b]). What does Fig. 13 teach us?

Smooth and broken transition from atom to bulk:

Clusters do behave like spherical conductive droplets if they have a size of $\gtrsim 20$ atoms. Their *IP*'s (and *EA*'s) correctly extrapolate to the bulk work function if the (trivial) electrostatic correction for curvature is applied. Hence, there is nothing dramatic happening from the atom to the bulk metal. The clusters are *gradually* assuming bulk-like metallic properties which are approximately reached at 50–100 atom size. The exception known today (and several more are to be expected) is Hg. Here a dramatic *nonmetal-metal* (Nm-M) *transition*[85] announces itself by a drop of the *IP* by more than 2 eV between 20 and 40 Hg atoms. A much more detailed experiment by *Bréchignac* et al.[86] with synchrotron radiation probing the ionization of an inner 5d electron reveals that Hg_x, $x < 10$, is a van der Waals aggregate with very small electronic coupling. The delocalization of electrons from the isolated atoms onto the whole cluster, i.e. the onset of metallic bonding, is observable from about Hg_{20} to Hg_{40} where it is practically finished in agreement with the drop in the *IP*'s. Of course, this behaviour was not unexpected. In fact *Tomanek, Mukherji* and *Bennemann* have predicted it several years ago[87], and *Hensel* et al. have a long experience with the properties of Hg near the critical point where a Nm-M transition is occurring in the expanded liquid phase[88]. Since $Hg(6s^2)$ is a noble gas like atom only van der Waals aggregates are expected and e.g. found in the dimer as shown in Section 4. Metallic bonding can only set in when the empty p orbitals participate in bonding (to simplify the argument!). Within the energy-band model of metals it involves overlap of the filled 6s-valence band with the empty 6p-band. With larger clusters, higher pressure, or both, this becomes true. However, how many atoms are necessary to reach this state, was not known. Estimates varied between several dozen and severeal thousand. Now it appears that what is necessary to create a metal from Hg atoms is decided at a cluster size of $\cong 50 \pm 20$ atoms. For the alkali metals and other metals with *partially filled* top electron levels formation of a conductance «band» does not require a critical size. The transition to the metal does not involve a break in properties as shown in Fig. 13.

Differences between cluster and bulk:

However, the small cluster differs from bulk by the small density of states near the Fermi level and thus by the discrete energy level system which creates a number of «quantum size» effect, i.e. the particles behave as normal molecules with a sparse distribution of filled and empty levels. Particularly the gap between the HOMO und LUMO is in the visible or near IR, i.e. large compared to kT, so optical, electrical, chemical ... properties will be widely different from a metal even though a completely delocalized system prevails from the onset, as demonstrated by the whole series of quantum chemical calculations on alkali metal and other clusters up to (M_{20} discussed in Section 4).

A cluster of these metals is only *quantitatively* different from a metal whereas small clusters of Hg (and other closed shell atoms) are *qualitatively* different.

They have to pass a discontinuity, the Nm-M transition, to become metals. This should be accompanied by a sudden increase in cohesive energy as well. No experimental information on this change is yet available.

Redoxpotentials of clusters:

Electronic differences between cluster and bulk, whether with or without Nm-M transition, will be reflected most strongly in chemical properties. Example: The changes in the *IP* will have direct effects on the redox potential. In order to express this, the gaseous *IP* has to be put into a thermochemical cycle where e.g. the solution reference state includes the free energy of solvation. To make use of the *IP*'s in Fig. 12:

		118.45		all numbers are ΔG_f^0 in kcal/mol
	Na	→	$Na^{\oplus}_{gas}$	
18.67	↑		↓	$\Delta G_{solv} = -199.71$ kcal/mol
	{Na}	→	$Na^{\oplus}_{aq}$	$E^0(Na^0/Na^{\oplus}_{aq}) = -3.52$ V (neglecting ΔG_{solv} of Na atom)
		−62.59		

With the other *IP*'s one obtains as a good estimate the following series of normal potentials:

E^0		[V]
$Na_1/Na^{\oplus}_{aq}$	=	−3.5
$Na_2/Na^{\oplus}_{2\,aq}$	=	-3.3_7
$Na_3/Na^{\oplus}_{3\,aq}$	=	−3.9[a])
$Na_4/Na^{\oplus}_{4\,aq}$	=	-3.3_5
...		...
$\{Na\}/Na^{\oplus}_{aq}$	=	−2.71[b])

[a]) Note the drop because the *IP* of Na_3 is so small, a «super alkali-metal» also in other reactions.
[b]) Bulk.

Series of this kind will be published elsewhere[107]. Of course, all the alkali metal clusters are unstable in water towards oxidation to $M^{\oplus}_{aq}$. Similar data have been used by *Henglein*[108] and *Calzaferri*[109] to deduce the redox potentials of the silver atom and of silver clusters, respectively.

Recently, *Belloni* et al.[110] have applied their own set of estimated redox potentials of *silver clusters* to describe the development process of silver photography for the first time in rational terms, i.e. relating to chemical particles involved. They have also been able to show that the redox potential of the developer discriminates, which cluster size makes an exposed emulsion grain developable. Since there is a drop in the redox potential between $Ag_2/Ag^{\oplus}_{2\,aq}$ to $Ag_3/Ag^{\oplus}_{3\,aq}$ similar to the one shown above for Na clusters, it is easily explainable, why more than 3 Ag atoms are necessary to make a stable developable silver speck. The Ag_3 «speck» will either be corroded in the developer (or before) or $Ag_3^{\oplus}$ will not be reduced because the redox pair with Ag_3 has a lower E^0 than the developer. However, Ag_4 will probably just work. This can easily be seen in the analogous and qualitatively similar plot for Na clusters in Fig. 12. So it seems that some old photographic phenomena will finally be explainable in a satisfactory way with the help of cluster chemistry.

The reader is, perhaps, surprised about how many deep inferences we draw from a crude model, the conductive droplet. We rely on its validity for the macroscopic system to which the cluster must extrapolate but have made use of many other facts, e.g. that these few atomic clusters at ambient temperature are probably all «molten» and thus nearly spherical (see end of Section 7).

The scatter at large $1/R$ in Fig. 13 shows that there are large quantum size effects for the smaller clusters. Whether the *IP* is a particularly sensitive observable for monitoring the evolution of a metal is questionable. However, it is the property which has been measured for the longest con-

tiguous cluster families to date. This is another important advantage of bare clusters compared to cluster complexes: The latter species are only available at those sizes which lead to stable preparations. Hence measurements of a property in a contiguous series of sizes is impossible. The experiments of *Bréchignac* et al.[86] yield more information than the simple *IP*'s are giving but its quantitative analysis is exceedingly difficult. It is interesting to predict, that the Nm-M transition as a function of cluster size should occur earlier than with Hg for Ba < Sr < Ca < Yb ≪ Mg ~ Mn and later for Eu ~ Be < Cd < Zn. No doubt, several of these transitions will be found in the near future. We assume that the ns-np energy gap is the decisive parameter.

Finally, it must be pointed out that excellent quantum mechanical predictions of the ionization potentials of alkali metal and other clusters with less than 14 atoms exist which reproduce the finer details averaged out by the spherical droplet model. They are in very good agreement with the measurements. Much insight into the bonding of metal clusters can be gained by studying those results[78]. However, no extrapolation to bulk can be made from them.

Less complete series of measurements exist for magnetic moments and for electrical polarizabilities. For a summary see Ref.[25b].

6. Cluster Populations, Discovery of Magic Numbers: The Canons and the Heathens

In Fig. 3 we showed the evolution of a Na-cluster population as a function of the Na partial pressure in an argon seeded expansion. We now investigate this size distribution generated under various conditions. When we first found such a *multimodal* distribution[15] in 1982 we observed, surprisingly, local intensity maxima among the Na_x at x = 2, 7 or 8, 19, 38, which were constant in x but variable in extent depending on seed gas (He, Ne, Ar, Kr, N_2). Before that experiment only unimodal distributions with exponential decay of cluster intensities towards higher x had been seen. Those were easily explainable with a crude nucleation model, but the new multimodal distributions not at all. Having made certain, that we had not been misled by all sorts of artefacts, we could think of (as discussed in Ref.[15] and some more) we accepted the distribution maxima as a sort of invariant characteristics of the system. The inference that the intensity maxima represent local abundance, hence partial pressure maxima in the mixture of clusters and thus reveal something about the *thermodynamic stability* of clusters is usually made uncritically by any newcomer to the cluster field. In 1984 the group of *Knight* with theoretical support of *Cohen* in Berkeley repeated this experiment[89], found also a multimodal intensity distribution, which showed slightly higher shifted maxima at x = 8, 20, 40, 58, 92 and immediately interpreted this as a distribution of the most stable clusters.

Electronic shell model of metal clusters:

The conviction with which they presented their case came from a model which allowed to generate these «magic numbers»: the nucleon shell model of the atomic nucleus (without spin-orbit coupling) which had served to deduce the nuclear magic (stability) numbers (with spin-orbit coupling) by *Goeppert-Meyer* and *Jensen* et al. 1949 translated to the electronic shell model of metal clusters. Since the nuclear shell model is a paradigm well known to every physicist (and to the radiochemists as well[90]) the acceptance of the Knight-Cohen shell model of metal clusters was an immediate and lasting success. Any criticism I might have is the outgrowth of pure jealousy! But in fact, it is worse: In 1977 I had already tried this model (not unknown to me because I had been a postdoc in Chicago 1954–1955, when *Maria Goeppert-Meyer* was there, and done radiochemistry in *Glenn Seaborg*'s laboratory in Berkeley, 1962, when spherical and deformed shell models were actively investigated by *Swiatecky* and others) for fitting the ionization potentials of Na_x und K_x clusters up to x = 14, without success (included 1978 in Ref.[80b], Fig. 8 and figure caption). Since the ionization potential is, in principle, such a simple observable I did not expect the model to work for the interpretation of more complex data like mass spectrometric abundances. Here I was wrong! However, before presenting the model, I come back to our 1982 experiment to show why I was wrong: We did not see 8, 20, 40, 58 ... but 7/8, 19, 38 ... as intensity maxima which prompted *Knight* in his paper to charge us with faulty mass spectrometry[89]. But as can be seen in Fig. 3, the evolution of a cluster population is strongly dependent on the formation conditions. Not even in the highest pressure expansion of Fig. 3e have we reached the «correct» magic numbers. We find 8, 19, 34 (!), 40 58, 68 (!) ..., so we still have 19 more abundant than 20, and find a prominent 34. Of course, we have long since learned, how to obtain the «canonical» magic numbers with or without seed gas, but nobody has ever defined the correct conditions to obtain them nor proven that the magic number distribution is a convergent cluster ensemble property which should be seen by every experimenter who does his job right. It is the other way round: The shell model is now believed so exclusively that experimenters withhold conflicting information from their publications, thus falsify the facts and hinder progress to a better understanding of the phenomena! So much for excuses of the heathens.

Electron in a spherical well:

Every student of chemistry hears several times the «particle in a linear box problem» of quantum mechanics, rarely the «particle in a 3-dimensional box», mentioned in Section 2, and probably never the «particle in a spherical well». But this is it! Here we come to our second crude model which is really also a warm-up exercise to be highly recommended for those who teach quantum chemistry courses: Take a metal cluster of n atoms with one valence electron each. Make a spherical droplet out of it with radius R_n, as in the first crude model (Section 5). Strip all the valence electrons and squeeze the n positive charges evenly into that sphere creating a uniform, positive background, called a jellium, a *mean field* approximation. Forget the volume the ion cores would have (imposed no less by *Pauli*'s exclusion principle!). Then take one electron, push it into the jellium, compute its one-particle eigenfunctions under the boundary conditions of the sphere and with the potential energy computed by integration of the Coulomb force between a volume element of the jellium background with a volume element of the electron charge density caused by the particular eigenfunction. In a cruder variant that potential is predefined with a simple but reasonable ansatz due to *Woods* and *Saxon*[91], parametrized with the ionization potential of the atom and the Fermi level of the bulk[89]. You then find a system of bound eigenvalues whose number grows with increasing size of the cluster or sphere. Now fill the n available electrons into it according to the «aufbau principle», i.e. obeying now *Pauli*'s principle and *Hund*'s rules. Count the number of electrons to create closed shells in different size clusters with multiplicity 1: You come up with:

number	2	8	18	20	34	40	58	68	70	92	...
shell	$1s^2$ +	$1p^6$ +	$1d^{10}$ +	$2s^2$ +	$1f^{14}$ +	$2p^6$ +	$1g^{18}$ +	$2d^{10}$ +	$3s^2$ +	$1h^{22}$	...
correct?	o.k.	o.k.	–	o.k.	–	o.k.	o.k.	–	(–)	o.k.	

The familiar symbols are connected with unfamiliar principle quantum numbers and in a strange order! This is the «nuclear» numbering scheme. Take $n' = n + l$ and you are back in normal water. However, the jellium sphere has an extended positive static spherical charge in contrast to the point charge of the proton. This makes the difference in the ordering of the levels. The jellium favours shells with high angular momentum, filling the sphere, the hydrogen atom those with high radial density being as close to the proton as compatible with the angular momentum. So this number sequence is the periodic system of metal clusters! With a slight hush: Several numbers generated do not appear as intensity maxima (–) or intensity breaks in the MS. But let us not be so fussy. We are happy with the coincidence of the majority of the numbers even though we do not have a good reason to suppress the rest.

Improved model:

Of course, the model can and has been made more sophisticated, even before it has been used by *Knight* et al.[92]. Leaving the jellium idea intact one can calculate a self-consistent model in which the electron- and the positive charge densities are allowed to adjust themselves optimally, electron-electron (but not ++) repulsion and simple electron correlation are introduced by *Ekardt*[92]. Interestingly, except perhaps for a reversal of some high-lying levels, and the suppression of the magic numbers 68, 70, which have never been observed by *Knight* (but see Fig. 3e), the top model is no better but no worse than the crudest one for predicting abundance maxima. Some other observables have been computed much better by the full model, e.g. polarizabilities. Now I had my triumph: For the *IP*'s up to Na_{22} the model still does not work better than 1977, as seen in Fig. 12 where both, the jellium prediction and the conductive droplet model are superimposed on the measured *IP*'s. This has also been remarked by *Ekardt*[92]. *Knight*'s group claims that the *IP*'s of K_x give a better fit than those for Na_x, especially for the larger clusters, but admit that the jellium shell closure exaggerates the drop in the *IP* after a magic number by a factor of 3. Nevertheless the breaks appear to be there, sometimes not entirely safe from the error bars. This has also been found by other authors (see Ref.[25b], p. 384). We admire the beautiful measurements of the Berkeley group, knowing how difficult they are.

What happens with the poor clusters which do not profit from a closed shell? In the spherical model they are left with terribly high multiplicities, are therefore rather unstable and should not be abundant, sic! Na_{27} is predicted to be an octet ground state with seven half-filled orbitals! Of course, such a system is absurd. It will immediately deform at least axially whereupon it has at most double degeneracy. *Clemenger*[93] has introduced another tool of the nuclear physicist, the Nilsson operator[94b] which allows for spheroidal deformations of the sphere to lift the degeneracies. His predictions of abundances between magic numbers using a deformed jellium are somewhat improved but not totally convincing if one compares the details of the predictions with the abundances. What does one want to interpret anyway, since the cluster abundances can be so easily shifted by the conditions of their formation, even the magic number positions?

The jellium model has served an important role: It has given a frame to discuss much larger clusters than those calculable by «good» quantum mechanics. Even more important was the introduction of awareness for electronic causes of stability. Earlier discussions of «magic numbers»[94b] had only considered packing or coordination stability. Finally, jellium calculations have an old tradition in condensed matter physics where they have been used for the discussion of many properties of large systems untreatable by quantum chemical methods. Thus a link of cluster physics with bulk physics through a simple (if not trivial) model using a mean field approximation has been opened.

In Fig. 14 we show the result of a simple, not self-consistent jellium calculation of Na-clusters with the above mentioned ansatz for the potential energy, similar to the one used in Ref.[80b]. In Section 7 an analogous calculation is presented for the heterocluster Na_8Mg with a composite Woods-Saxon potential.

So much about crude models, which have their every day merit but should not be preached with religious zeal. How do we proceed from here?

Magic numbers as a consequence of the formation history:

We have not yet adressed the processes responsible for variations in abundance distributions which have occupied our laboratory in recent years. By changing the nozzle geometry from cylindrical to conical one obtains in a neat (unseeded) expansion all the canonical magic numbers[95]. With the other parameters of the cluster formation process one can shift neighbour abundances almost at will and thus detect, whether every mass peak is a genuine representative of the neutral precursor particle. It turns out that many MS intensities M_n^+ are contaminated by fragmentation of the n + 1 particle[96]. This enhances certain peaks and depletes others. The magic numbers m are both enhanced by fragments of the less stable m + 1 particle but they fragment themselves contributing to a too high intensity of the m − 1 peak. For the ions two fragmentation patterns, the m→m − 1 and m→m − 2 channel have been found and modelled[97]. All this is now fairly well in hand since mass spectra are taken, as a consequence of these results, at minimal excess energy of 0.1 to 0.5 eV above the ionization threshold and checked for intensity changes caused by ionization in this range. Apart from this ionization-induced unimolecular cluster decay thermal unimolecular decay can occur. This is linked to the question whether the observed cluster distributions constitute macrocanonical ensembles in the sense of *Gibbs*, i.e. whether they are thermodynamic properties. The clear answer is: No. The observed abundances, if free from artefacts, are the product of a *formation history*. It is probable, but not proven, that conditions exist to produce cluster «ensembles» of reasonably convergent distributions which could be stated in communicable terms and reproduced by every laboratory. We are not yet

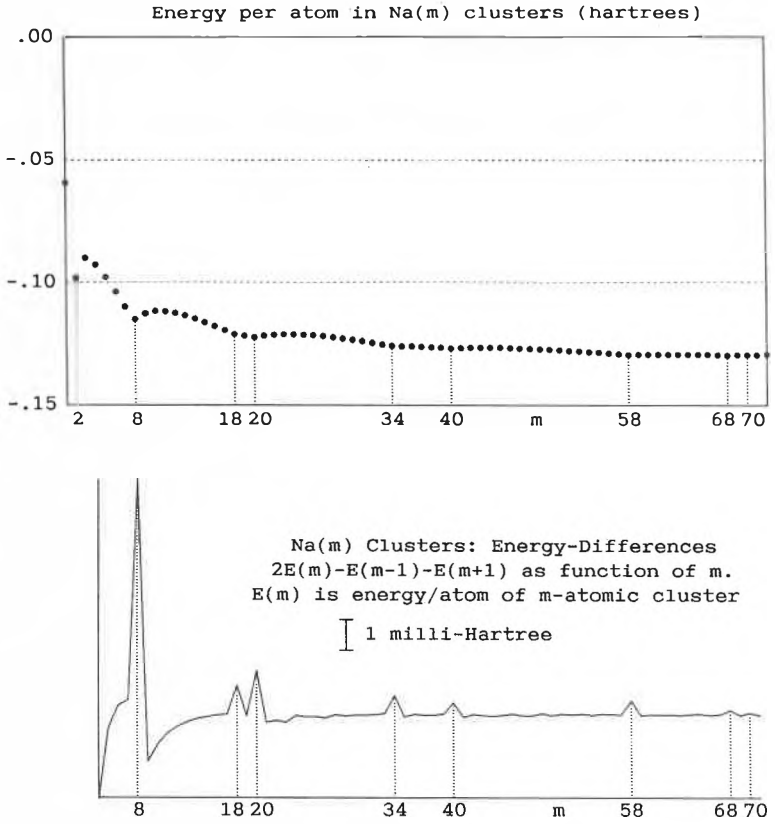

Fig. 14. Upper part: Jellium mean field calculation of the energy per Na atom in a cluster Na_m as a function of m (as computed by E. S. 1977 [80b]). The lower part shows the same information using the second difference of these energies in order to enhance the tiny changes marked in the upper part (kind of plot introduced by Knight et al.[89]). This allows to accentuate the closed shell changes happening at m = 8, 18, 20, 34, 40, and much weaker at 68, 70. The last two dips disappear in a self-consistent calculation. Smaller wiggles in between the peaks are spurious and vanish for higher precision of the calculated eigenvalues.

there. If that goal is reached one could start talking about «magic numbers» as particles of preferred thermodynamic stability and model them with decent theories, but not now. We have shown with Na-clusters that the «canonical» distribution, i.e. that distribution which exhibits the same magic numbers as observed by *Knight*, contains widely varying temperatures of the individual clusters in the range 200–500 K. The temperature distribution is linked to the abundance pattern[98]. Another important insight into these questions derives from the observation of thermally generated random distributions and segregation of Li/Na[99] and Na/K mixed clusters[100].

The questions raised will be answerable by more realistic models of clusters than those used hitherto. The temperature-driven dynamics has to be part of the model. It is fortunate that such methods are now becoming available. A beautiful example is the *ab initio* molecular dynamics treatment of Na- and NaK-clusters by *Ballone, Andreoni, Car,* and *Parinello*[101]. They make understandable the segregation of Na to the centre of a 20-atom NaK cluster. This shows that important technical processes linked to *sintering* can be modelled on the decisive microsopic scale of the problem. The stability of the cluster follows other boundary conditions than that of the macroscopic bulk because surface free energy is a dominant quantity. Therefore, heterometallic compositions can easily be made which do not represent bulk alloy thermodynamics to the extent that macroscopically immiscible phases become homogeneously dispersed. Li and Na are not miscible beyond mole fractions of 0.005 for either metal. However, we were able to show that M_{20} becomes more and more stable traversing the series Li_xNa_{20-x} from $x = 0$ to $x = 10$[99]. From the molecular dynamics simulations of *Ballone* et al.[101] for NaK-clusters we expect a segregation of a few percents of Li and Na such that Li prefers the centre, Na the periphery of the cluster. This is in the direction of phase separation but this will never go to completion within such a tiny system. Similar high miscibility has been observed in many other seemingly immiscible macroscopic metals. Making such «exotic» cluster compositions, quenching the clusters at low temperature, and sintering them together at medium temperature where the cluster surfaces will merge may lead to a totally new class of «cluster-materials» not accessible by thermodynamically controlled metallurgy. They have new properties and can thus dramatically enlarge the repertoire for manufacturing metallic objects.

7. Glimpse at Ongoing Work, Problems, Applications

7.1. Metal-Metal Bond Coordination Chemistry

In a way the free cluster chemistry reveals the molecular or coordination chemistry of the metallic bond.

In the best of chemical traditions but partially corrupted by quantum chemistry a chemical bond can best be studied between *different* atoms. In order to learn something about the stability and selectivity of the metal-metal bond interactions heteroclusters have to be made and investigated, of course without ligands. We expect, as with the homonuclear clusters, to obtain an abundance distribution of species with varying composition which will exhibit local maxima. The persistence of these can be probed under varying composition of the feeding phases. This will, hopefully, lead to abundance ≅ concentration variations from which we can deduce stability criteria. The strategy is the same as the well-known solution chemists vademecum. However, we have more tools to probe the species, see Section 3. In addition to those mentioned we can now directly probe dissociation channels kinetically and energetically in any single cluster and thus obtain stability data without the doubtful detour over thermodynamic relations.

Our first goal is to understand the onset of bonding partition of empty p-orbitals in ns^2 atoms. This is akin to finding the Nm-M transition in systems of *different* atoms. Our present data base includes the coordination chemistry of group 2a, 2b and some transition metal atoms as central atoms with Na and K used as ligands.

These particles differ from traditional coordination chemistry in that they have only metal bonds and that the interactions between the ligand atoms are of comparable strengths of those between central atom and ligand.

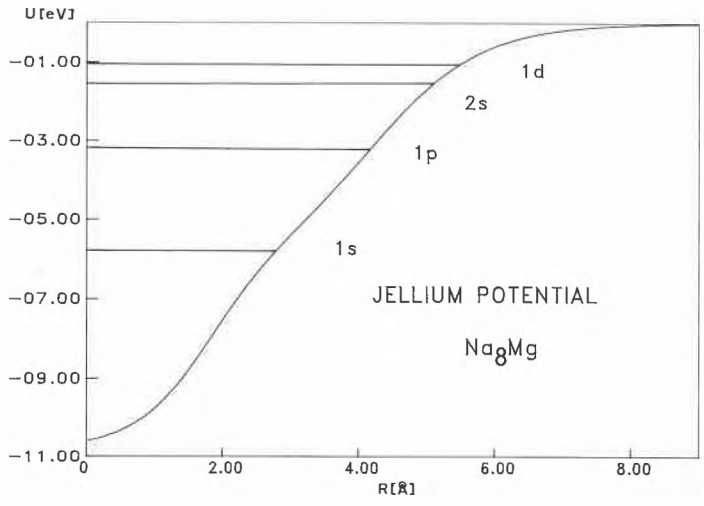

Fig. 15. Jellium potential and eigenvalues plotted for Na_8Mg using the following parameters for the Woods-Saxon potential: $U_o(Na) = 5.98$ eV; $U_o(Mg) - U_o(Na) = 4.81$ eV; $ep(Na) = 1.5$; $ep(Mg) = 1.0115$; $r(Na) = 2.08$ Å; $r(Mg) = 1.77$ Å. Using the «aufbau» principle one arrives at $1s^21p^62s^2$, i.e. a closed shell for this 10 electron particle as predicted[182]*. A cubic structure is compatible with computations performed with Extended Hückel Theory (EHT) as well as with ab initio SCF/CI. The jellium calculations only assume a central Mg and 8 peripheral Na in spherical symmetry which is equivalent to a cube.*

Fig. 15 shows a jellium calculation of Na_8Mg where the levels are plotted in the Woods-Saxon well composed of the parameters of Mg in the centre and of Na towards the periphery. This is identical with the assumption that Na_8Mg forms a Mg-centred «spherical» system. Since 8 discrete particles do not span a sphere the only coordination polyhedron where the 8 ligands are equivalent is a cube. We see that the canonical jellium level sequence 1p-1d-2s has been reversed by the central Mg which has a higher ionization potential than Na. The new sequence 1p-2s-1d allows for a 10 electron closed shell system, which is represented, now for K_8Mg which is similar, in Fig. 16 by an abundance maximum. EHT calculations also give a cubic structure and the same is true for ab initio MC-SCF-CI results obtained by *Koutecký* (personal communication). More interesting is the ensemble of species formed. No bonding interaction is descernible below K_5Mg. Bonding starts at K_6Mg to reach its local optimum at K_8Mg. Beyond 8, abundances sharply drop to reach a second maximum at $K_{18}Mg$ with 20 electrons and probably a Mg-centred octahedron (1-4-8-4-1 layers with $8+8$ nearest neighbours for Mg). At K_6Mg we already have full participation of the p-orbitals, hence metallic interaction. Below K_5Mg probably only van der Waals aggregates exist, unobserved in these experiments. The ionization potentials proved to be the key to understand the electronic structure. We use Fig. 15 also for discussing K_6Mg since the level sequence is not changed. This conforms to the canonical magic number $1s^21p^6$ (which is also the old noble

gas closed shell!). The ionization potential of this complex is predicted to be higher than that of K_8Mg and that is exactly what the experiment finds (Fig. 17). So we have a good case to postulate the filling of a new shell between those two species[102].

This sample may suffice for now. We have information on all group 2a, 2b Na, K-complexes except for Be[103]. Interesting differences in selectivity at the 6-7-8- and 16-17-18-19 coordination numbers are revealed which correlate with space filling, ns-np gap energy, and ionization potential difference between central atom and ligand. In all these complexes the central atom assumes a negative polarization which can grow to 0.5–0.8 electron charges as computed by EHT. This creates Madelung stabilization which helps to «crystallize» these complexes in high symmetry in contrast to the homonuclear species which have very little internal polarizations.

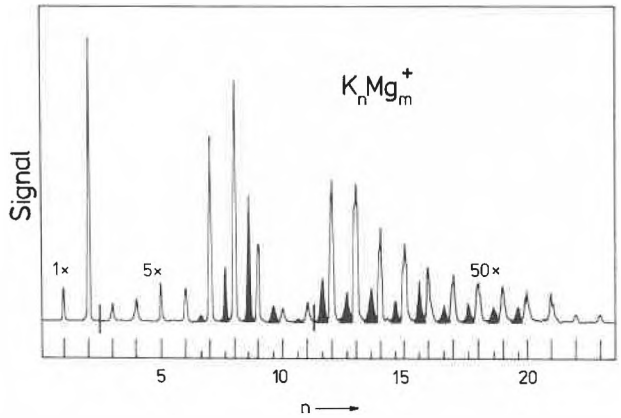

Fig. 16. Formation of K_nMg_m in the K_n cluster family by coexpansion of the vapours of both metals. The abscissa gives the number n of K atoms in the pure K-cluster drawn with open peaks for m = 0. The filled peaks are K-clusters with m = 1 Mg atom. No second Mg atom is incorporated at the experimental conditions used which gave a very low mole fraction for Mg. The first mixed cluster appears as K_6Mg with an 8 electron closed shell. The most stable one is K_8Mg the 10 electron system treated for Na_8Mg in Fig. 15.

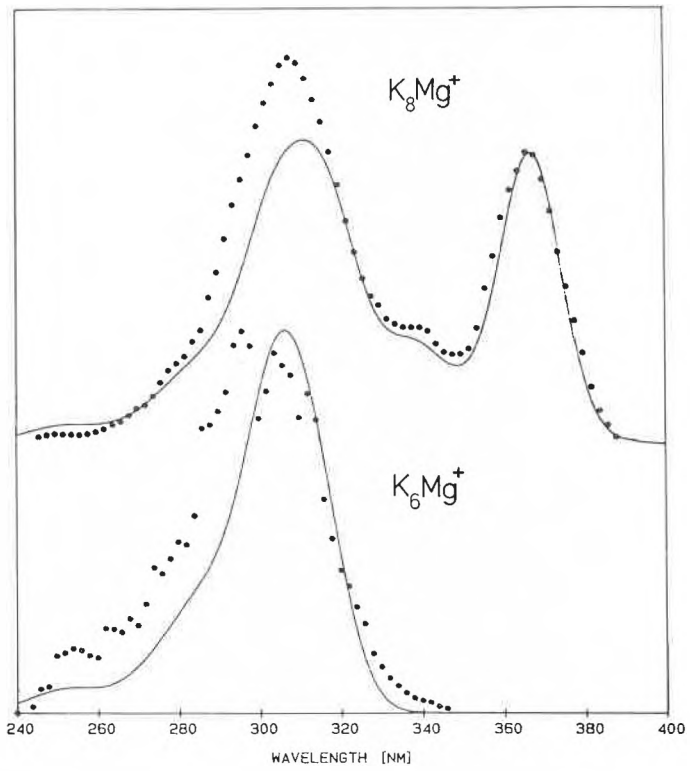

Fig. 17. Photoionization efficiency curves measured for K_8Mg and K_6Mg with monochromator and using a Xe-Hg high pressure lamp. The dots are ion currents in the two mass windows, the smooth curves are fits to the data under the assumption that the ionization threshold can be modelled by a step function (this is a different assumption than that used in evaluating the data in Fig. 11 and Fig. 12. It does, however not influence the conclusions). The long-wavelength thresholds are about 50 nm apart, i.e. the smaller complex needs 0.4 eV more energy to ionize than the larger. This difference together with the preponderant stability of K_8Mg proves that a new shell has been built going form 6 to 8 potassium ligands for Mg. This effect occurs similarly with Ca, Sr, Ba, Zn, Cd, Hg, Eu, Yb in K-ligated clusters, i.e. with ns^2 central atoms. In all these cases K_8M is more stable than K_6M but has a lower ionization potential. This agrees with the calculation for the analogous Na_8Mg shown in Fig. 15.

7.2. Metal Clusters in Zeolites

Since many years we have been fascinated by the interaction of alkali metals with dry zeolites. Caesium metal is spontaneously sorbed by zeolite Y when the molten metal comes into contact with this aluminosilicate. A strongly coloured pigment is formed whose reflection spectrum depends on amount of sorbed and removable cations present in the zeolite lattice. Inspection shows a totally nonmetallic sorbate which on heating desorbs all the metal to form a mirror on the walls of the containing vessel. Homogeneous colouring of the zeolite crystal powder and of the crystal inner volume is compatible with the assumption of a dispersion of the metal into approximately equal size clusters sitting at comparable postitions within the zeolite. That is also borne out by ESR investigations which show discrete clusters of 4 or 6 atoms. With higher metal content the sytem becomes darker and finally black. It reveals now the onset of a metallic electronic system by showing the metal-like resonances akin to Pauli magnetism.

EHT calculation proves the interpretation of the absorption spectrum as cluster-lattice charge transfer. This fact strongly mediates the chemical behaviour of these molecular metal dispersions. They behave less strongly reductive than the bulk metal and thus produce easily controllable chemical reactions, e.g. Wurtz-Fittig coupling of halogenohydrocarbons. They also initiate the anionic radical chain growth of polymers from α-olefins thus forming a polyethylene microwrap of the zeolite crystals and a non-separable composite of a polymer with an inorganic porous matrix, a model system which can easily be generalized[104]. Beautiful applications of Ag-clusters in zeolites for experiments to study the conversion of solar photonic energy into chemical storage have been developed over the last years by *Calzaferri* and his collaborators[109].

7.3. Problems: The State of Aggregation of Metal Clusters

Partitioning a solid into smaller and smaller pieces withdraws among other physical changes lattice cohesion energy. This has a direct consequence for the solid-liquid phase transition, see references in Ref.[25b]. It has been predicted by extrapo-

lation from larger sizes that the melting point of Au-clusters is less than 400 °C at the 100 Å size, falling rapidly below. The extrapolation to less than 100 atoms invariably leads to «molten» clusters at temperatures of 100–300 K. What that term implies becomes blurred at this size: Does melting scale into the vibrational motion of the small finite system or is there something more fundamental involved which translates into a large-scale sudden coherent ordering/disordering phenomenon? This question is now a hot research topic in several laboratories, e.g. *Berry*[111] and *Leutwyler* in our institute[105]. How do these phenomena change with cluster size and temperature? It is important to have a cluster thermometer to attack this problem. We now have a reasonably good approximation to such a tool. The floppy molecule which undergoes large amplitude motion is the model system to start with. Its description transcends the normal coordinate analysis in rigid point groups. The best methodology is modelling with the tools of molecular dynamics. This is carried out by *Leutwyler* and his collaborators on transputers and the Cray machines for van der Waals clusters.

A more practical question pertains to the structure controversy: Why must a cluster have shape? They probably don't have shape at temperatures of several dozen Kelvin and up. Hence, the mean field approximation of the jellium model is not as bad as it looks, although no thermal, phononic component is, as yet, incorporated. Electron diffraction is not very revealing, because it just announces the occurrence of bulk atomic distances when the clusters become larger and larger. That is, however, to be expected. Clusters have to be frozen to a few Kelvins in order to reveal shape. How could it be determined in a particle specific fashion? *Leutwyler* knows how to do it for van der Waals clusters. For metal clusters several other ideas have to be tested. Using heterometallic clusters with transition-metal centres should allow to observe ligand-field splittings of the d- or f-electrons in absorption and emission spectra as well as their consequences in the magnetic moment of the complexes. These experiments reveal the rigid point group. First attempts to observe these effects in the fluorescence of K_xEu have not yet been successful because of low abundance. Now we have several 3d-TM-metal complexes under study which can be observed in absorption in a particle selective way. The idea is to make use of the transition metal centre as an electronic probe for structure.

Shapelessness as a generic property of *homonuclear* metal clusters at finite temperature scales into malleability and ductility of the macroscopic bulk metal. *Heterometallic* clusters are more rigid and preserve shape to higher temperatures akin to the effect of alloying in metallurgy. This is yet another incidence of the emergence of macroscopic properties at the molecular level where they can be interpreted in terms of the interactions of the atomic building units.

We have now touched all metallic properties mentioned at the start and their correspondence with the realm of clusters. Since we also know fairly well how to model clusters starting with the atom, the bridge has been built to link the atom to the bulk.

Acknowledgment: We should like to thank Prof. Dr. Manfred M. Kappes, Chemistry Department, Northwestern University, Evanston IL, for this contributions to many problems mentioned in this review; Prof. Dr. Gion Calzaferri for his development of an EHT extension treating nuclear repulsion explicitely, thus allowing realistic structure optimizations, and for his program; René Bühler for drawings and photography, Urs Bill for hardware, and Mrs. F. Bornhauser for secretarial help.

Received: October 21, 1988 [FR 60]

[1] B.B. Mandelbrot: *The Fractal Geometry of Nature*, Freeman, New York (1983).
[2] R. Boyle: *The Sceptical Chymist* (1661), reprinted by Dent, London, Everyman's Library (1949), p. 30, 31.
[3] A.W. Castleman Jr., R.G. Keesee, *Acc. Chem. Res. 19* (1986) 413; see also Ref.[25b], p. 372.
[4] A. Herrmann, S. Leutwyler, E. Schumacher, L. Wöste, *Helv. Chim. Acta 61* (1978) 453.
[5] Cf. e.g. *4th International Symposium on Small Particles and Inorganic Clusters*, 5–9 July (1988) Aix-Marseille, book of abstracts.
[6] J.C. Phillips (AT&T Bell Laboratories), *Chem. Rev. 86* (1986) 619. Very active metal and semiconductor cluster research is also going on at Exxon Research (A. Kaldor et al.), Annandale NJ; Eastman-Kodak, Rocherster NY; General Electric, Schenectady NY; and other companies active in materials science, catalysis, and devices. Furthermore US government laboratories are involved, especially Argonne National Laboratory, Chicago.
[7] W.D. Knight, W.A. de Heer, W.A. Saunders, K.C. Clemenger, M.Y. Chou, M.L. Cohen, *Chem. Phys. Lett. 134* (1987) 1; M.M. Kappes, M. Schär, P. Radi, E. Schumacher, *J. Chem. Phys. 84* (1986) 1863.
[8] See e.g. chapter 23 in: F.A. Cotton, G. Wilkinson, *Advanced Inorganic Chemistry, 5th Ed.*, Wiley-Interscience, New York (1988).
[9] G. Schmid, *Struct. Bonding (Berlin) 62* (1985) 51; M.P.J. van Staveren, H.B. Brom, L.J. de Jongh, G. Schmid, paper A 69 in *4th International Symposium on Small Particles and Inorganic Clusters*, 5–9 July (1988) Aix-Marseille, book of abstracts.
[10] A. Müller, J. Döring, H. Bögge, E. Krickemeyer, *Chimia 42* (1988) 300.
[11] L. Pauling: *The Nature of the Chemical Bond*, Cornell University Press, Ithaca (1945), chapter 11, p. 401.
[12] See e.g. C. Kittel: *Einführung in die Festkörperphysik, 3. Aufl.*, Oldenbourg, München (1973).
[13] a) H. Beck, H.-J. Güntherodt, in *Glassy Metals I*, Springer, Berlin (1981), p. 1–17; b) Proc. 6th Int. Conf. *Liquid and Amorphous Metals (LAM 6)*, ed. W. Gläser, F. Hensel, E. Lüscher, Oldenbourg, München (1987); c) J. Parenboom, P. Wyder, F. Meier, *Phys. Rev. 78* (1981) 173.
[14] A. Meyer, *Z. Phys. Chem. (Frankfurt am Main) 156* (1988) 519.
[15] See e.g. Ref.[4] and M.M. Kappes, R.W. Kunz, E. Schumacher, *Chem. Phys. Lett 91* (1982) 413; M.M. Kappes, S. Leutwyler, in G. Scoles (Ed.): *Atomic and Molecular Beam Methods, Vol. 1*, Oxford University Press, Oxford (1987).
[16] M. Hoffmann, Ph.D. thesis, Universität Bern (1980), p. 60.
[17] F. Blatter, E. Schumacher, *J. Less-Common Met. 115* (1986) 307.
[18] M.G. Inghram, J. Drowart in: Int. Symp. *High Temperature Technology*, Asilomar, October 6 (1959), p. 338; K.A. Gingerich, *Faraday Symp. Chem. Soc. 14* (1980) 109; K.A. Gingerich, in E. Kaldis (Ed.): *Current Topics in Materials Science*, Vol. 6, North-Holland, Amsterdam (1980).
[19] Li_3: C.H. Wu, *J. Chem. Phys. 65* (1976) 3181; Li_4: *J. Phys. Chem. 87* (1983) 1543; Li_5: *J. Chem. Phys.*, in press.; K. Hilpert, *Ber. Bunsenges. Phys. Chem. 88* (1984) 260.
[20] O. Hagena, in P. Wegener (Ed.): *Molecular Beams and Low Density Gas Dynamics*, Dekker, New York (1974).
[21] D.M. Lubman, C.T. Rettner, R.N. Zare, *J. Phys. Chem. 86* (1982) 1129.
[22] G. Schmid, *Nachr. Chem. Tech. Lab. 34* (1987) 249. This paper abounds with misunderstandings regarding the experimental work with bare clusters, its significance, and the motivation for it. In the fifties the Bjerrum-Schwarzenbach-Sillén school of solution chemists was exposed to similar misunderstandings from the preparative chemists of their time. Our statement is, however, not meant to criticize the important and fascinating new cluster chemistry, Schmid and his colleagues have discovered.
[23] See e.g. P. Fayet, L. Wöste, *Z. Phys. D3* (1986) 177.
[24] See e.g. W. Stumm, J.J. Morgan: *Aquatic Chemistry, 2nd ed.*, Wiley, New York (1981).
[25] a) We have stated the idea in Ref.[4] and elaborated it in *Ber. Bunsenges. Phys. Chem. 88* (1984) 220; b) see also M.M. Kappes, *Chem. Rev. 88* (1988) 369–389.
[26] Ref.[25b], p. 289–301; also Ref.[7].
[27] See e.g. M.M. Kappes, M. Schär, U. Röthlisberger, C. Yeretzian, E. Schumacher, *Chem. Phys. Lett. 143* (1988) 251; D. Leopold, J. Ho, W. Lineberger, *J. Chem. Phys.*, in press.
[28] D.L. Feldman, R.K. Lengel, R.N. Zare, *Chem. Phys. Lett. 52* (1977) 413; A. Herrmann, S. Leutwyler, E. Schumacher, L. Wöste, *ibid. 52* (1977) 418.
[29] S. Wülfert, D. Herren, S. Leutwyler, *J. Chem. Phys. 86* (1987) 3751; J. Barnes, T. Gough, *Chem. Phys. Lett. 130* (1986) 297; T. Gough, D. Knight, G. Scoles, *ibid. 97* (1983) 155.
[30] K.H. Bowen, in Ref.[5], p. 12; G. Ganteför, K.H. Meiwes-Broer, H.O. Lutz, *Phys. Rev. A 37* (1988) 2716; Ref.[5], p. 11.
[31] a) M. Hofmann, Ph.D. thesis, Universität Bern (1980); M. Hofmann, H.-P. Härri, K.O. Marti, E. Schumacher, MS measurements (1980), to be published; b) D.M. Cox, D.H. Trevor, R.L. Whetten, E.A. Rohlfing, A. Kaldor, *Phys. Rev. B32* (1985) 7290.
[32] W.D. Knight, K. Clemenger, W. de Heer, W. Saunders, *Phys. Rev. B31* (1985) 2539; A.A. Lushnikov, A.J. Somonov, *Phys. Lett. 44A* (1973) 45.
[33] U. Röthlisberger, M. Schär, E. Schumacher, submitted to *Z. Phys. D*; see U. Röthlisberger, Diploma thesis, Universität Bern, May (1988).
[34] M.M. Kappes, M. Schär, E. Schumacher, A. Vayloyan, *Z. Phys. D5* (1987) 359; C. Bréchignac, P. Cahuzac, J.-P. Roux, *J. Chem. Phys.*, in press.
[35] M.M. Kappes, M. Schär, E. Schumacher, to be published.
[36] M. Geusic, M. Morse, R. Smalley, *J. Chem. Phys. 82* (1985) 590; R.L. Whetten, D.M. Cox, D.H. Trevor, A. Kaldor, *Phys. Rev. Lett. 54* (1985) 1494; S. Richtsmeier, E. Parks, K. Liu, K. Pobo, S. Riley, *J. Chem. Phys. 82* (1985) 3659.
[37] M.M. Kappes, M. Schär, U. Heiz, A. Vayloyan, E. Schumacher, to be published.
[38] J. Farges, M.F. Feraudy, B. Raoult, G. Torchet, in J. Jortner et al. (Ed.): *Large Finite Systems*, Jerusalem Symposium on Quantum Chemistry, May 11–14 (1987), Reidel, Dordrecht, p. 113.
[39] E. Blaisten-Barojas, I.L. Garzon, M. Avalos, *ibid.* p. 241.
[40] a) E.P. Kündig, M. Moskovits, G.A. Ozin, *Nature (London) 254* (1975) 503, and many papers of G.A. Ozin et al. in *Inorg. Chem.*; *J. Am. Chem. Soc.* (1975–1980); also M. Hofmann, S. Leut-

wyler, W. Schulze, *Chem. Phys. 40* (1979) 145; M. Moskovits, G. Ozin (Ed.): *Cryochemistry*, Wiley, New York (1979); – b) D.M. Lindsay, D.R. Herschbach, A.L. Kwiram, *Mol. Phys. 32* (1976) 1199; G.A. Thompson, D.M. Lindsay, *J. Chem. Phys. 74* (1981) 959.

[41] V.E. Bondybey, J.H. English, *J. Chem. Phys. 74* (1981) 6978; and especially D.E. Powers, S.G. Hansen, M.E. Geusic, A.C. Pulu, J.B. Hopkins, T.G. Dietz, M.A. Duncan, P.R.R. Langridge-Smith, R.E. Smalley, *J. Phys. Chem. 86* (1982) 2556.

[42] C_{60} etc., described in several papers by R.E. Smalley et al., as told by R.M. Baum, *Chem. Eng. News 66* (1988) 33.

[43] S.C. O'Brien, Y. Liu, Q. Zhang, J.R. Heath, F.K. Tittel, R.F. Curl, R.E. Smalley, *J. Chem. Phys. 84* (1986) 4074.

[44] M. Jarrold, J. Bower, *J. Chem. Phys. 85* (1986) 5373.

[45] F. Frank, W. Schulze, B. Tesche, J. Urban, B. Winter, *Surf. Sci. 156* (1985) 90.

[46] O. Echt, K. Sattler, E. Recknagel, *Phys. Rev. Lett. 47* (1981) 1121; J. Mühlbach, K. Sattler, P. Pfau, E. Recknagel, *Phys. Lett. 87A* (1982) 415, 418.

[47] P.S. Skell, L.D. Weston Jr., *J. Am. Chem. Soc. 85* (1963) 1023; P.L. Timms, *ibid. 89* (1967) 1629.

[48] G.A. Ozin, H. Huber, *Inorg. Chem. 17* (1978) 155; *18* (1979) 1402.

[49] G. Schwarzenbach: *Allgemeine und Anorganische Chemie, 4. Aufl.* Thieme, Stuttgart (1950), p. 64.

[50] M.M. Kappes, K.O. Marti, P. Radi, M. Schär, E. Schumacher, *Chem. Phys. Lett. 107* (1984) 6.

[51] W. Müller, W. Meyer, *J. Chem. Phys. 80* (1984) 3311; L. v. Szentpaly, P. Fuentalba, H. Preuss, H. Stoll, *Chem. Phys. Lett. 93* (1982) 555; W. Stevens, D. Konowalov, L. Ratcliff, *J. Chem. Phys. 80* (1984) 1215.

[52] M.M. Kappes, M. Schär, E. Schumacher, *J. Phys. Chem. 89* (1985) 1499.

[53] N.W. Ashcroft, *Z. Phys. Chem. (Frankfurt am Main) 156* (1988) 41.

[54] Data on diatomics are most complete in: K. Huber, G. Herzberg, *Molecular Spectra and Molecular Structure, IV. Constants of Diatomic Molecules*, Van Nostrand, New York (1979).

[55] G. Verhaegen, S. Smoes, J. Drowart, *J. Chem. Phys. 40* (1964) 239.

[56] L.B. Knight Jr., R. Van Zee, W. Weltner Jr., *Chem. Phys. Lett. 94* (1983) 296.

[57] See summary by M.D. Morse, *Ber. Bunsenges. Phys. Chem. 88* (1984) 228.

[58] B. Delley, *Phys. Rev. Lett. 55* (1985) 2090; *50* (1983) 488.

[59] I. Shim, K.A. Gingerich, *J. Chem. Phys. 77* (1982) 2490.

[60] M.J. Pelissier, *J. Chem. Phys. 75* (1981) 775; *79* (1983) 2099.

[61] H. Eyring, M. Polanyi, *Z. Phys. Chem. B12* (1931) 279.

[62] G. Calzaferri, *Chem. Phys. Lett. 87* (1982) 443.

[63] G. Herzberg, *J. Chem. Phys. 70* (1979) 4806.

[64] See Ref.[28] and E. Schumacher, W.H. Gerber, H.-P. Härri, M. Hofmann, E. Scholl, in J.L. Gole, W.C. Stwalley (Ed.): *Metal Bonding and Interactions in High Temperature Systems, ACS Symp. Ser. 179* (1982) 83; S. Leutwyler, A. Herrmann, L. Wöste, E. Schumacher, *Chem. Phys. 48* (1980) 253; S. Leutwyler, M. Hofmann, H.-P. Härri, E. Schumacher, *Chem. Phys. Lett. 77* (1981) 257; S. Leutwyler, T. Heinis, M. Jungen, E. Schumacher, *J. Chem. Phys. 76* (1982) 4290.

[65] E. Scholl (1976), Ph.D. thesis, Universität Bern (1980), p. 102–120; later R.L. Martin, E.R. Davidson, *Mol. Phys. 35* (1978) 1713.

[66] A. Herrmann, M. Hofmann, S. Leutwyler, E. Schumacher, L. Wöste, *Chem. Phys. Lett. 62* (1979) 216.

[67] M. Broyer, G. Delacrétaz, P. Labastie, R.L. Whetten, J.P. Wolf, L. Wöste, *Z. Phys. D3* (1986) 131; *Phys. Rev. Lett. 57* (1986) 1851; G. Delacrétaz, E. Grant, R. Whetten, L. Wöste, J. Zwanziger, *Phys. Rev. Lett. 56* (1986) 2598.

[68] P. Radi, M.M. Kappes, E. Schumacher, submitted for publication (1988); P. Radi, Ph.D. thesis, Universität Bern (1986), p. 72–84. In the same thesis very much improved spectra in comparison to the first paper[66] have been measured for Na_3 band system A, shown in Fig. 8.

[69] L. Wöste, talk at *Summerschool in Cluster Science*, G. Scoles dir., July (1988) Varenna, to be published.

[70] W.H. Gerber, E. Schumacher, *J. Chem. Phys. 69* (1978) 1692; corrected and improved computation: W.H. Gerber, Ph.D. thesis «Theorie des dynamischen Jahn-Teller-Effekts in Li_3 und Untersuchung von Lithium-Molekularstrahlen», Universität Bern (1980). The corrected Jahn-Teller potential surface E_- is shown in Fig. 6.

[71] H.C. Longuet-Higgins, U. Öpik, M.H.L. Pryce, R.A. Sack, *Proc. R. Soc. London Ser. A 244* (1958) 1; see also I.B. Bersuker: *The Jahn-Teller Effect and Vibronic Interactions in Modern Chemistry*, Plenum Press, New York (1984); R.L. Whetten, G.S. Ezra, E. Grant, *Annu. Rev. Phys. Chem. 36* (1985) 277–320; G. Herzberg: *Molecular Spectra and Molecular Structure, III. Electronic Spectra and Electronic Structure of Polyatomic Molecules*, Van Nostrand, New York (1966), p. 20–65.

[72] The *«adiabatic sign-change theorem»*, cf. H.C. Longuet-Higgins, *Adv. Spectrosc. 2* (1961) 429. This can be visualized with a computer animation of the pseudorotating triangle: The eye may be deceived into interpreting that movement as the motion of an *equilateral* triangle *in space*, intersecting the plane of the three atoms. The corners move along a spiral up and down around every atom location which has 4π as an identity operation. The moving intersection of the triangle with the atom plane exactly traces the node of the vibronic wave function. To be published with computer program in *J. Chem. Educ.*

[73] F. Cocchini, T.H. Upton, W. Andreoni, *J. Chem. Phys. 88* (1988) 6068.

[74] See Ref.[31a].

[75] W.A. de Heer, A.R. George, W.H. Gerber, W.D. Knight, «Magnetism of Alkali Trimers», preprint of a paper (1981).

[76] W.H. Gerber, personal communication (1981).

[77] T. Sears, T.A. Miller, V.E. Bondybey, *J. Chem. Phys. 72* (1980) 6070.

[78] I. Boustani, W. Pewestorf, P. Fantucci, V. Bonačić, J. Koutecký, *Phys. Rev. B35* (1987-II) 9437; J. Koutecký, P. Fantucci, *Chem. Rev. 86* (1986) 538 and many preceding papers cited therein.

[79] X-ray structure: E. Weiss, E.A.C. Lucken, *J. Organomet. Chem. 2* (1964) 197; E. Weiss, G. Hencken, *ibid. 21* (1970) 265; D.P. Novak, T.L. Brown, *J. Am. Chem. Soc. 94* (1972) 3793. – Theory: J.B. Collins, J.D. Dill, E.D. Jemmis, Y. Apeloig, P. von R. Schleyer, R. Seeger, J.A. Pople, *ibid. 98* (1976) 5419 and many more papers of P. von R. Schleyer et al., e.g. *ibid. 98* (1976) 4332; *99* (1977) 6159; *Tetrahedron Lett. 17* (1976) 3923.

[80] Early *IP*-measurements on alkali metal clusters: a) R. Leckenby, E. Robbins, P. Trevalion, *Proc. R. Soc. London Ser. A 280* (1964) 408; E. Robbins, R. Leckenby, P. Willis, *Adv. Phys. 16* (1967) 739; P. Foster, R. Leckenby, E. Robbins, *J. Phys. B2* (1969) 478; b) A. Herrmann, L. Wöste, E. Schumacher, *J. Chem. Phys. 68* (1978) 2327; c) K. Peterson, P. Dao, R. Farley, A.W. Castleman Jr., *J. Chem. Phys. 80* (1984) 1780. – Modern TOF measurements all in Ref.[5]: T. Bergmann, H. Limberger, N. Malinowski, T.P. Martin, H. Schaber, B. Wassermann, p. 24; H.G. Limberger, T.P. Martin, p. 120; N. Malinowski, T.P. Martin, p. 144.

[81] However see Ref.[7, 26, 80c].

[82] M.M. Kappes, M. Schär, U. Röthlisberger, C. Yeretzian, E. Schumacher, *Chem. Phys. Lett. 143* (1988) 251.

[83] J. Smith, *Am. Inst. Aeronaut. Astronaut. Eng. 3* (1965) 648; D. Wood, *Phys. Rev. Lett. 46* (1981) 749. These two derivations are mathematically correct but, perhaps, physically unrealistic for the distance of a few 100 pm from the «surface» of the metallic droplet. A more physical approach, supported by jellium calculations, arrives at a slope of $\frac{1}{2}$ instead of $\frac{3}{8}$: A.J. Nitzan, *J. Chem. Phys.*, submitted for publication; see also M. van Staveren, H. Brom, L. de Jongh, Y. Ishii, *Phys. Rev. B35* (1987) 7749; however a slope of $\frac{1}{2}$ is at variance with all the experimental information which supports slopes of 0.33–0.39 but not at all 0.5. The reason given by Nitzan for the discrepancy of his derivation from experiment is an unspecified quantum mechanical effect. This is not plausible, because the smaller slope is mainly supported by the largest clusters being nearest to bulk behaviour.

[84] K. Rademann, B. Kaiser, U. Even, F. Hensel, *Phys. Rev. Lett. 59* (1987) 2319.

[85] N.F. Mott, *Can. J. Phys. 34* (1956) 1356; *Philos. Mag. 6* (1961) 287; *Rev. Mod. Phys. 40* (1968) 673; Philos. Mag. 37 (1978) 377; *Metal-Insulator Transitions*, Taylor and Francis, London (1974).

[86] C. Bréchignac, M. Broyer, P. Cahuzac, G. Delacrétaz, P. Labastie, L. Wöste, *Chem. Phys. Lett. 120* (1985) 559; C. Bréchignac, personal communication (1987) on Hg_{20} to Hg_{40}.

[87] D. Tomanek, S. Mukherji, K.H. Bennemann, *Phys. Rev. B28* (1983) 665.

[88] F. Hensel, in J. Jortner et al. (Ed.): *Large Finite Systems*, Reidel, Dordrecht (1987), p. 345 and references therein.

[89] W.D. Knight, K. Clemenger, W.A. de Heer, W.A. Saunders, M.Y. Chou, M.L. Cohen, *Phys. Rev. Lett. 52* (1984) 2141.

[90] B.G. Harvey: *Introduction to Nuclear Physics and Chemistry*, Prentice-Hall, Englewood Cliffs (1962), p. 86ff.

[91] R.D. Woods, D.S. Saxon, *Phys. Rev. 95* (1954) 577.

[92] J.L. Martins, R. Car, J. Buttet, *Surf. Sci. 106* (1981) 265; D.E. Beck, *Solid State Commun. 49* (1984) 381; W. Ekardt, *Phys. Rev. B29* (1984) 1558.

[93] K. Clemenger, *Bull. Am. Phys. Soc. 30* (1985) 423.

[94] a) O. Echt, K. Sattler, E. Recknagel, *Phys. Rev. Lett. 47* (1981) 1121; b) S.G. Nilsson, *K. Dan Vidensk. Sels. Mat. Fys. Medd. 29* (1955), No. 16.

[95] M.M. Kappes, M. Schär, E. Schumacher, *J. Phys. Chem. 91* (1987) 658.

[96] M.M. Kappes, M. Schär, E. Schumacher, A. Vayloyan, *Z. Phys. D5* (1987) 359.

[97] C. Bréchignac, personal communication; *J. Chem. Phys.* (1988), in press.

[98] U. Röthlisberger, M. Schär, E. Schumacher, submitted for publication.

[99] M.M. Kappes, P. Radi, M. Schär, C. Yeretzian, E. Schumacher, *Z. Phys. D3* (1986) 115; M.M. Kappes, M. Schär, E. Schumacher, *J. Phys. Chem. 91* (1987) 658.

[100] C. Bréchignac, personal communication.

[101] P. Ballone, W. Andreoni, R. Car, M. Parrinello, *Phys. Rev. Lett.*, in press.

[102] M.M. Kappes, P. Radi, M. Schär, E. Schumacher, *Chem. Phys. Lett. 119* (1985) 11; *Chimia 39* (1985) 187. The statement in both papers, that the lower *IP* of K_8Mg is incompatible with the higher overall stability as demonstrated by the much higher abundance in comparison to K_6Mg is not verified when the jellium calculation is actually performed, as shown in Fig. 15.

[103] C. Yeretzian, M. Schär, E. Schumacher, submitted for publication.

[104] F. Blatter, E. Schumacher, *Surf. Sci. 203* (1988) 571 and references therein; K.W. Blazey, K.A. Müller, F. Blatter, E. Schumacher, *Europhys. Lett. 4* (1987) 857.

[105] S. Leutwyler, J. Bösiger, *Faraday Discuss. Chem. Soc. 86* (1988) 1–16.

[106] F. Blatter, T. Irlet, M. Haldimann, E. Schumacher, U. Zauner, to be published in *Chimia*.

[107] E. Schumacher, submitted for publication.

[108] A. Henglein, *Ber. Bunsenges. Phys. Chem. 81* (1977) 556.

[109] G. Calzaferri, *Chimia 40* (1986) 74; B. Sulzberger, G. Calzaferri, *J. Photochem. 19* (1982) 321; G. Calzaferri, S. Hug, T. Hugentobler, B. Sulzberger, *ibid. 26* (1984) 109; G. Calzaferri, W. Spahni, *ibid. 32* (1986) 151; S. Leutwyler, E. Schumacher, *Chimia 31* (1977) 475.

[110] J. Belloni, personal communication (October 26, 1988): J. Belloni, M. Mostafavi, J.L. Marignier, J. Amblard, 3ieme Reunion dans le cadre du PICS CNRS/FN, Bern (1988), paper given by J. Belloni.

[111] R.S. Berry, in J. Avery et al. (Ed.): *Understanding Molecular Properties*, Reidel, Dordrecht (1987), p. 425–448.